Table 1
Summary of patients treated with bevacizumab.

Case	Age	Gender	Disease	After 1 cycle			After 2–5 cycles			Overall survival	
				MacDonald criteria	RANO criteria	HBDW criteria	MacDonald criteria	RANO criteria	HBDW criteria	Months	Current status
1	47	F	Glioblastoma rec.	CR	PD	PD	PD	PD	PD	5.0	Dead
2	42	F	Glioblastoma rec.	PR	PR	PD	PD	PD	PD	3.3	Dead
3	65	M	Glioblastoma rec.	SD	SD	SD	PD	PD	PD	6.1	Dead
4	45	M	Glioblastoma rec.	CR	CR	PR	CR	CR	PR	19.1	Alive
5	37	M	Glioblastoma rec.	PR	PR	PR	CR	CR	PR	5.8	Alive
6	43	M	Anaplastic astrocytoma rec.	CR	CR	PR	CR	CR	CR	30.2	Alive
7	65	F	Anaplastic astrocytoma rec.	PR	PR	PD	SD	SD	PD	6.2	Dead
8	13	F	PNET rec.	PD	PD	PD	PD	PD	PD	3.1	Dead
9	37	M	Pontine glioma rec.	CR	SD	SD	PD	PD	PD	2.3	Dead
10	6	F	Pontine glioma rec.	PR	SD	SD	PD	PD	PD	2.0	Dead

RANO, response assessment in neuro-oncology working group; HBDW, high *b*-value diffusion-weighted; rec., recurrence; PNET, primitive neuroectodermal tumor; CR, complete response; PR, partial response; SD, stable disease; PD, progressive disease.

There is an apparent increase in the tendency for infiltrating tumor progression after anti-angiogenic treatment; this is discernible on T2-weighted- and FLAIR images [14]. This may be attributable to the recruitment of existing blood vessels. Under RANO criteria, the most recent response criteria for glioma, T2/FLAIR images are taken into account [2]. However, other factors, e.g. post-irradiation- and/or postoperative changes, chemotherapy, tumor infiltration, and tumor-induced edema, may produce changes on T2-weighted- or FLAIR images, pointing to the need for clear response criteria.

Newer imaging techniques such as PET, MR spectroscopy, and perfusion- and diffusion-weighted imaging that provide functional information may be more reliable in the assessment of tumor activity during anti-angiogenic treatment [2]. Tumor-cell density decreases if treatment is effective. On the other hand, ineffective treatment or tumor recurrence results in increased tumor-cell density and the size of the high cell density area increases due to an increase in the tumor size [7].

Ours is the first documentation that HBDW (*b*-4000) imaging at MRI more effectively distinguishes between pseudo- and true responses than other MRI techniques including standard *b*-1000 DW imaging. HBDW imaging has been found to be useful for the diagnosis of acute infarction [9], degenerative diseases [10], for glioma grading [11], and for the differentiation between glioblastoma and malignant lymphoma [12]. Preclinical studies using HBDW support our findings that HBDW may be useful for the early detection of responses to chemotherapy [15]. At HBDW there is more contrast at the tissues of interest than at regular *b* value imaging [16] and it has been reported that there are slow- and fast diffusion components that correspond with intra- and extracellular

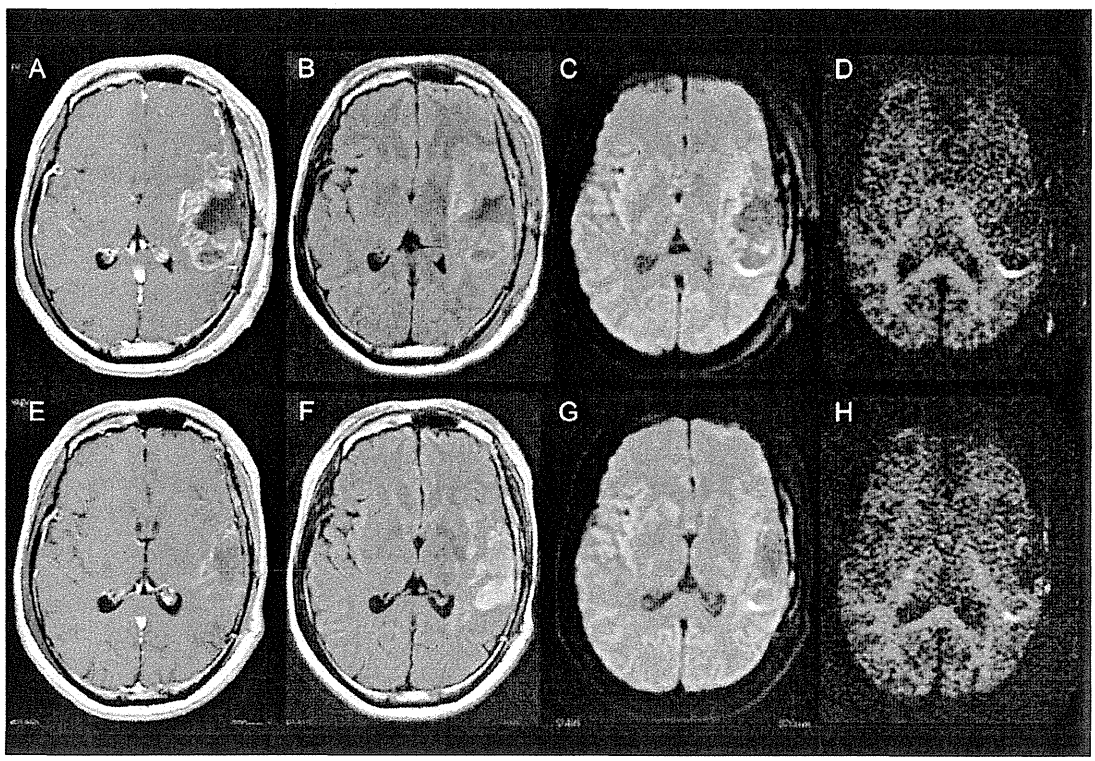

Fig. 1. This 37-year-old man with glioblastoma underwent radical surgery and radiotherapy with concomitant and adjuvant chemotherapy with temozolomide. Gadolinium (Gd)-enhanced T1-weighted- (A) and FLAIR images (B), DW images at *b*-1000 s/mm^2 (DWI_{1000}) (C) and at *b*-4000 DWI (DWI_{4000}) (D) were acquired before treatment with bevacizumab. Gd-enhanced T1-weighted images showed a marked decrease in the enhanced lesion (E). On FLAIR images (F), DWI_{1000} (G), and DWI_{4000} (H) the high intensity area was decreased. At present, 6 months post-treatment, there has been no tumor recurrence and he continues to receive bevacizumab treatment.

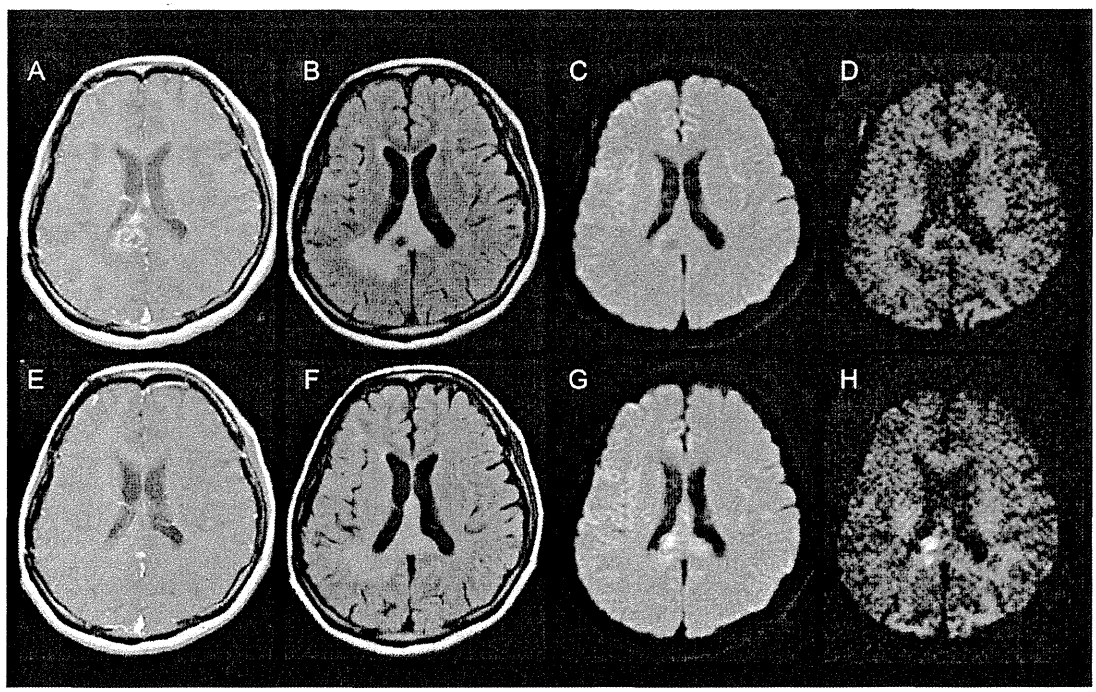

Fig. 2. This 47-year-old woman with glioblastoma underwent radical surgery and radiotherapy with concomitant and adjuvant chemotherapy with temozolomide. Gd-enhanced T1-weighted- (A) and FLAIR images (B) and DWI_{1000} (C) and DWI_{4000} (D) were acquired before treatment with bevacizumab. Gd-enhanced T1-weighted images showed a marked decrease in the enhanced lesion (E). On FLAIR images (F) and DWI_{1000} (G) and DWI_{4000} (H) the high-intensity area was increased. She died of tumor recurrence 5 months after the first course of bevacizumab.

diffusion, respectively [17,18]. Studies on multi-component diffusion in brain tissue demonstrated that the slow component is more sensitive at HBDW- than regular *b*-value DW imaging, suggesting that the ADC based on higher *b*-values reflects changes in tumor cellularity more accurately [12]. In fact, Doskaliyev et al. [12] found that the ADC is inversely associated with tumor cellularity and that this correlation is stronger with the ADC obtained at HBDW (*b*-4000) than regular b value DW (*b*-1000) imaging.

Calculation of the ADC should also be considered for the assessment of the tumor response. However, the ADC is associated with tumor cellularity but not with the tumor size. A decrease in cellularity after effective treatment would result in an increase in the ADC.

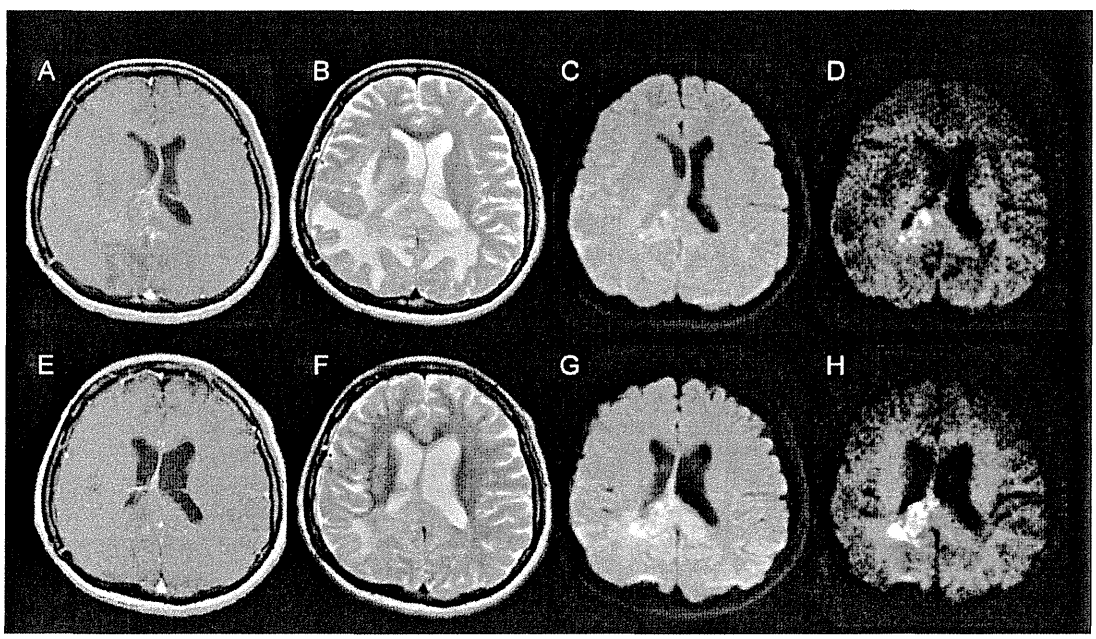

Fig. 3. This 42-year-old woman with glioblastoma underwent radical surgery and radiotherapy with concomitant and adjuvant chemotherapy with temozolomide. Gd-enhanced T1-weighted- (A) and T2-weighted images (B) and DWI_{1000} (C) and DWI_{4000} (D) were acquired before bevacizumab treatment. Gd-enhanced T1-weighted images showed a marked decrease in the enhanced lesion (E). On T2-weighted images we noted a marked decrease in the high intensity area, a decrease in the mass effect, and improvement in the midline shift (F). DWI_{1000} showed an increase in the high intensity area (G). On DWI_{4000} there was an obvious increase in the high-intensity area (H). She died of tumor recurrence 3 months after first course of bevacizumab.

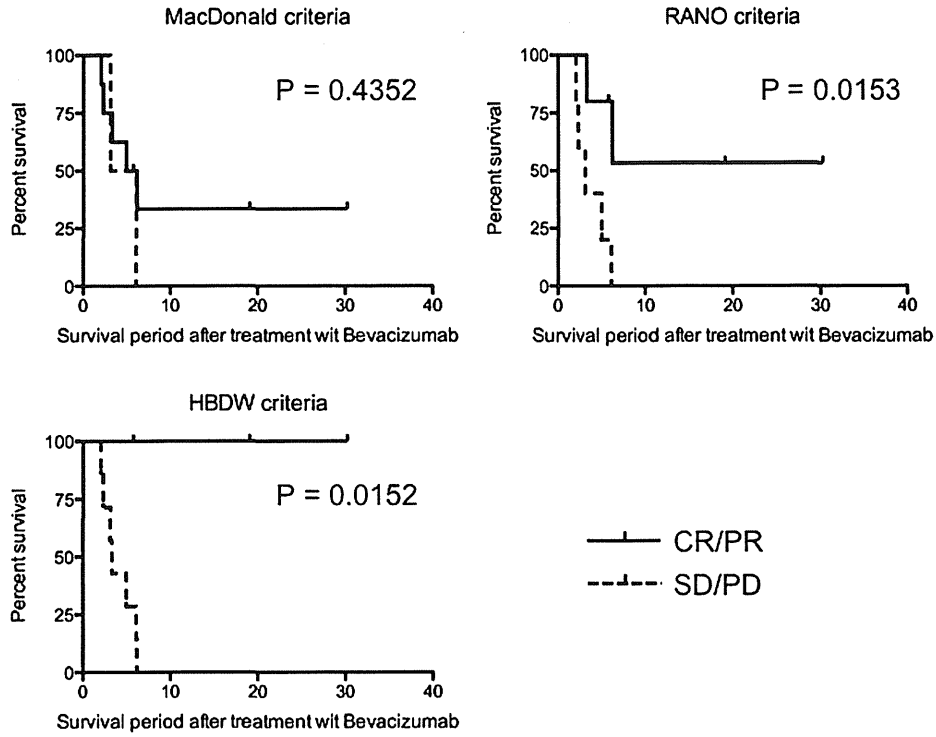

Fig. 4. Kaplan–Meier survival curves of all patients with recurrent glioma treated with bevacizumab (including 3 who remain alive) show the relationship between the evaluation criteria and the survival time measured from the date of surgery. Comparisons were between patients with complete response (CR)/partial response (PR) and stable disease (SD)/progressive disease (PD) using MacDonald criteria (A), between CR/PR and SD/PD using RANO criteria (B), and between CR/PR and SD/PD using DWI criteria.

However, calculation of the ADC at identical tumor sites before and after treatment is difficult. Moreover, it would be difficult to interpret changes in the ADC without evaluating the size of the tumor. In addition, use of the terms hyper- and hypocellularity instead of decreasing ADC and increasing ADC may be misleading since many pathologies and clinical scenarios affect ADC measurements.

The quantification of diffusion changes has evolved from the mean change in the ADC to a voxel-by-voxel approach termed the functional diffusion map (fDM) [7], a statistical method that prospectively compares heterogeneous ADC maps acquired after the start of therapy with pretreatment ADC maps. The two image data sets are co-registered and computationally analyzed to yield statistical maps of ADC changes as color overlays on anatomical images and to provide scatter plots of ADC changes to determine the tumor response in patients with brain tumors. Such information makes it possible to tailor treatments based on an early imaging biomarker readout in cases where an insufficient response is predicted. The fDM was proposed as an MRI biomarker for the quantification of the early brain tumor response to therapy [19].

Although the fDM approach is promising, technical and clinical challenges must be addressed [20]. First, the proper alignment of sequential images on baseline images is difficult but critical. A significant mass effect from tumor growth or intracranial pressure induced by edema may skew the registration between DW imaging datasets. Suspected tumor regions near gyri, sulci, or the ventricles may return false results due to misregistration effects. The proper choice of the *b*-value used for an accurate estimation of the ADC is an important aspect of fDM implementation that must be addressed. Also, the use of *b*-values greater than 1500 s/mm^2 results in a multi-exponential signal decay that may render a single estimate of the ADC inappropriate. Additional studies are necessary to confirm the usefulness of the fDM approach.

Our preliminary study has some limitations. First, we must consider that acute occlusion of the tumor vessels may produce high intensity on DW images. Time-course observations and monitoring of ADC changes may help to identify pseudo-responses. Second, although HBDW (*b*-4000) imaging was superior to regular *b* value-based (*b*-1000) DW imaging for the assessment of pseudo-response at visual inspection, HBDW imaging had the disadvantage of an inferior signal/noise ratio, and it may be possible to assess pseudo-responses by regular *b*-value DWI. Quantitative analysis that includes the tumor ADC value or the fDM approach is necessary to confirm the advantage of HBDW. In addition, the optimal *b*-value has not been determined. Third, tumors with lower cellularity and tumors with micro-necroses or micro-cysts may not show high intensity on HBDW images. Fourth, in our study the patients' age and the tumor histology were inhomogeneous. Fifth, the 6-mm slice thickness we used may be too high for an accurate assessment of the character of the lesion. Thinner slices may make it possible to characterize the lesions more accurately. Sixth, our study population was small and prospective studies on large patient populations, studies to identify the optimal *b*-value, and studies that include quantitative approach are necessary.

In conclusion, HBDW criteria could identify a pseudo-response earlier than RANO criteria. We presented evidence that HBDW imaging may represent a biomarker in glioma patients subjected to anti-angiogenic therapy.

Conflict of interest

None.

Acknowledgements

We thank Ursula Petralia for editorial review. This study was partially supported by the grant-in-aid for Japan Society for the Promotion of Science Grant-in-Aid for Scientific Research (C) Nos. 22591612 and 23592091.

Appendix A. Supplementary data

Supplementary data associated with this article can be found, in the online version, at doi:10.1016/j.ejrad.2011.10.018.

References

[1] Pope WB, Lai A, Nghiemphu P, Mischel P, Cloughesy TF. MRI in patients with high-grade gliomas treated with bevacizumab and chemotherapy. Neurology 2006;66(8):1258–60.

[2] Wen PY, Macdonald DR, Reardon DA, et al. Updated response assessment criteria for high-grade gliomas: response assessment in neuro-oncology working group. J Clin Oncol 2010;28(11):1963–72.

[3] Vredenburgh JJ, Desjardins A, Herndon 2nd JE, et al. Phase II trial of bevacizumab and irinotecan in recurrent malignant glioma. Clin Cancer Res 2007;13(4):1253–9.

[4] Vredenburgh JJ, Desjardins A, Herndon 2nd JE, et al. Bevacizumab plus irinotecan in recurrent glioblastoma multiforme. J Clin Oncol 2007;25(30):4722–9.

[5] Sugahara T, Korogi Y, Kochi M, et al. Usefulness of diffusion-weighted MRI with echo-planar technique in the evaluation of cellularity in gliomas. J Magn Reson Imaging 1999;9(1):53–60.

[6] Padhani AR, Liu G, Koh DM, et al. Diffusion-weighted magnetic resonance imaging as a cancer biomarker: consensus and recommendations. Neoplasia 2009;11(2):102–25.

[7] Moffat BA, Chenevert TL, Lawrence TS, et al. Functional diffusion map: a noninvasive MRI biomarker for early stratification of clinical brain tumor response. Proc Natl Acad Sci USA 2005;102(15):5524–9.

[8] Yamasaki F, Sugiyama K, Ohtaki M, et al. Glioblastoma treated with postoperative radio-chemotherapy: prognostic value of apparent diffusion coefficient at MR imaging. Eur J Radiol 2010;73(3):532–7.

[9] Cihangiroglu M, Citci B, Kilickesmez O, et al. The utility of high *b*-value DWI in evaluation of ischemic stroke at 3 T. Eur J Radiol 2011;78:75–81.

[10] Yoshiura T, Mihara F, Tanaka A, et al. High *b* value diffusion-weighted imaging is more sensitive to white matter degeneration in Alzheimer's disease. Neuroimage 2003;20(1):413–9.

[11] Seo HS, Chang KH, Na DG, Kwon BJ, Lee DH. High *b*-value diffusion ($b = 3000$ s/mm^2) MR imaging in cerebral gliomas at 3 T: visual and quantitative comparisons with $b = 1000$ s/mm^2. AJNR Am J Neuroradiol 2008;29(3):458–63.

[12] Doskaliyev A, Yamasaki F, Ohtaki M, et al. Lymphomas and glioblastomas: differences in the apparent diffusion coefficient evaluated with high *b*-value diffusion-weighted magnetic resonance imaging at 3 T. Eur J Radiol 2010;(December) [Epub ahead of print].

[13] Macdonald DR, Cascino TL, Schold Jr SC, Cairncross JG. Response criteria for phase II studies of supratentorial malignant glioma. J Clin Oncol 1990;8(7):1277–80.

[14] Norden AD, Drappatz J, Wen PY. Novel anti-angiogenic therapies for malignant gliomas. Lancet Neurol 2008;7(12):1152–60.

[15] Roth Y, Tichler T, Kostenich G, et al. High-*b*-value diffusion-weighted MR imaging for pretreatment prediction and early monitoring of tumor response to therapy in mice. Radiology 2004;232(3):685–92.

[16] Mardor Y, Roth Y, Ochershvilli A, et al. Pretreatment prediction of brain tumors' response to radiation therapy using high *b*-value diffusion-weighted MRI. Neoplasia 2004;6(2):136–42.

[17] DeLano MC, Cooper TG, Siebert JE, Potchen MJ, Kuppusamy K. High-*b*-value diffusion-weighted MR imaging of adult brain: image contrast and apparent diffusion coefficient map features. AJNR Am J Neuroradiol 2000;21(10):1830–6.

[18] Niendorf T, Dijkhuizen RM, Norris DG, van Lookeren Campagne M, Nicolay K. Biexponential diffusion attenuation in various states of brain tissue: implications for diffusion-weighted imaging. Magn Reson Med 1996;36(6):847–57.

[19] Pope WB, Young JR, Ellingson BM. Advances in MRI assessment of gliomas and response to anti-VEGF therapy. Curr Neurol Neurosci Rep 2011;11(3):336–44.

[20] Ellingson BM, Malkin MG, Rand SD, et al. Validation of functional diffusion maps (fDMs) as a biomarker for human glioma cellularity. J Magn Reson Imaging 2010;31(3):538–48.

European Journal of Radiology 81 (2012) 1863–1869

Contents lists available at ScienceDirect

European Journal of Radiology

journal homepage: www.elsevier.com/locate/ejrad

Role of perfusion-weighted imaging at 3 T in the histopathological differentiation between astrocytic and oligodendroglial tumors

Taiichi Saito[a,*], Fumiyuki Yamasaki[a], Yoshinori Kajiwara[a], Nobukazu Abe[b,1], Yuji Akiyama[b], Takako Kakuda[b], Yukio Takeshima[c,2], Kazuhiko Sugiyama[a], Yoshikazu Okada[d,3], Kaoru Kurisu[a]

[a] Department of Neurosurgery, Hiroshima University, 1-2-3 Kasumi, Minami-ku, Hiroshima 734-8551, Japan
[b] Department of Clinical Radiology, Hiroshima University, 1-2-3 Kasumi, Minami-ku, Hiroshima 734-8551, Japan
[c] Department of Pathology, Hiroshima University, 1-2-3 Kasumi, Minami-ku, Hiroshima 734-8551, Japan
[d] Department of Neurosurgery, Tokyo Women's Medical University, 8-1 Kawada, Shinjuku-ku, Tokyo 162-8666, Japan

ARTICLE INFO

Article history:
Received 4 January 2011
Accepted 5 April 2011

Keywords:
Perfusion imaging
Magnetic resonance imaging
Oligodendroglioma
Astrocytoma
Glioma

ABSTRACT

Objective: The differentiation of oligodendroglial tumors from astrocytic tumors is important clinically, because oligodendroglial tumors are more chemosensitive than astrocytic tumors. This study was designed to clarify the usefulness of 3 T MR perfusion imaging (PWI) in the histopathological differentiation between astrocytic and oligodendroglial tumors. This is because there is a growing interest in the diagnostic performance of 3 T MR imaging, which has the advantages of a higher signal-to-noise ratio (SNR) and greater spatial and temporal resolution.

Materials and methods: This study retrospectively included 24 consecutive patients with supratentorial, WHO grade II and III astrocytic and oligodendroglial tumors (7 astrocytic, 10 oligoastrocytic, and 7 oligodendroglial tumors) that were newly diagnosed and resected between November 2006 and December 2009 at Hiroshima University Hospital. These patients underwent dynamic susceptibility contrast-enhanced (DSC) PWI relative cerebral blood volume (rCBV) measurements before treatment. Astrocytic tumors were designated as the astrocytic group, and oligoastrocytic and oligodendroglial tumors as the oligodendroglial group. The regions of interest with the maximum rCBV values within the tumors were normalized relative to the contra-lateral white matter (rCBVmax).

Results: The average rCBVmax of astrocytic tumors (2.01 ± 0.68) was significantly lower than that of the oligoastrocytic (4.60 ± 1.05) and oligodendroglial tumors (6.17 ± 0.867) ($P < 0.0001$). A cut-off value of 3.0 allowed to differentiate the oligodendroglial group from the astrocytic group at 100% sensitivity and 87.5% specificity.

Conclusion: The rCBVmax values obtained from 3 T MR PWI may be useful as an adjunct to the postoperative histopathological diagnosis of glioma patients.

1. Introduction

The differentiation of gliomas containing oligodendroglial components from astrocytic tumors is important clinically, because oligodendroglial and oligoastrocytic tumors are more chemosensitive than astrocytic tumors [1]. However, the differentiation of these tumors is sometimes difficult, because of the ambiguous criteria. Although a histopathological evaluation remains the reference standard for the histological subtyping of gliomas, this method is limited by issues such as subjective criteria, heterogeneity within tumors, and tissue sampling errors. Attempts have been made to enhance the prognostic information obtained by the histological classification of gliomas. Therefore, additional supportive information is required histopathological classification. Recently, dynamic susceptibility contrast-enhanced (DSC) MR perfusion imaging (PWI) has been used as part of a combined approach with histopathology in order to help to accurately subtype brain tumors [2,3].

There is evidence that MR PWI may be a sensitive marker of the microvascular density in gliomas. Relative cerebral blood volume (rCBV) measurements are closely correlated with angio-

* Corresponding author. Tel.: +81 82 257 5227; fax: +81 82 257 5229.
E-mail addresses: t-saitou@qc4.so-net.ne.jp (T. Saito), fyama@hiroshima-u.ac.jp (F. Yamasaki), kaji@hiroshima-u.ac.jp (Y. Kajiwara), abebe@hiroshima-u.ac.jp (N. Abe), uakiyama@hiroshima-u.ac.jp (Y. Akiyama), taka4121@hiroshima-u.ac.jp (T. Kakuda), ykotake@hiroshima-u.ac.jp (Y. Takeshima), brain@hiroshima-u.ac.jp (K. Sugiyama), yokada@nij.twmu.ac.jp (Y. Okada), kuka422@hiroshima-u.ac.jp (K. Kurisu).
[1] Tel: +81 82 257 5257.
[2] Tel: +81 82 257 5152; fax: +81 82 257 5154.
[3] Tel: +81 3 3353 8111; fax: +81 3 5269 7438.

0720-048X/$ – see front matter © 2011 Elsevier Ireland Ltd. All rights reserved.
doi:10.1016/j.ejrad.2011.04.009

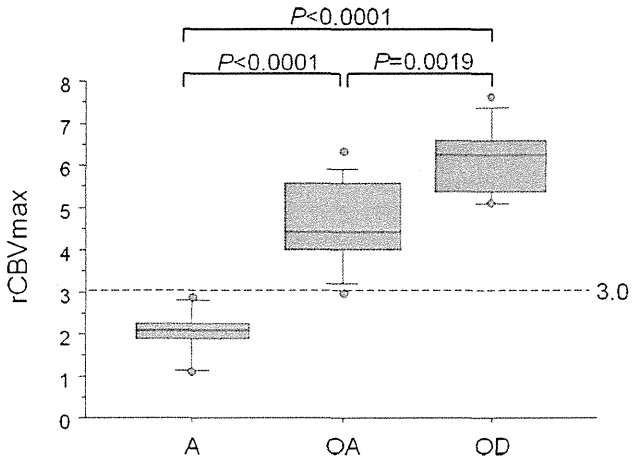

Fig. 1. Box plots of rCBVmax values for astrocytic tumors, oligoastrocytic tumors, and oligodendroglial tumors along with their respective standard deviation values. The cut-off line of 3.0 yields 100% sensitivity and 87.5% specificity for differentiating the oligodendroglial group (oligoastrocytic tumors and oligodendroglial tumors) from the astrocytic group. A, astrocytic tumors; OA, oligoastrocytic tumors; OD, oligodendroglial tumors.

graphic and histologic markers of tumor vascularity [4]. Perfusion image-based brain tumor characterization is currently performed by assessing the maximum ratio between an rCBV area within the glioma and the unaffected contralateral rCBV value (rCBV-max) [5]. Oligodendrogliomas often have an attenuated network of branching capillaries resembling a chicken wire pattern. Most oligodendroglial tumors (oligodendrogliomas and oligoastrocytomas) exhibit higher rCBVmax values than astrocytic tumors [3].

Some reports have demonstrated the usefulness of PWI in the assessment of hemodynamics in gliomas and differentiation of oligodendroglial tumors from astrocytic tumors [3]. However, these reports used 1.5 T MR imaging, and significant overlaps of rCBV-max values were observed between astrocytic and oligodendroglial tumors. Recently, with the integration of 3 T imaging into clinical practice, there is a growing interest in the diagnostic performance of 3 T MR imaging techniques with respect to the established magnetic field strength of 1.5 T [6,7]. MR performed at higher magnetic field strengths has the advantages of higher signal-to-noise ratio (SNR) and magnetic susceptibility; this results in improved spatial and temporal resolution [6,7]. Therefore, these advantages may help improve the accuracy of differential diagnoses of gliomas. Therefore, this study was designed to characterize the hemodynamics within gliomas by using 3 T MR PWI and clarify whether this approach help the postoperative histopathological diagnosis in the differentiation between astrocytic and oligodendroglial tumors.

2. Materials and methods

2.1. Patients and histological diagnosis

This study retrospectively included 24 consecutive patients with supratentorial, WHO grade II and III astrocytic and oligodendroglial tumors that were newly diagnosed and resected between November 2006 and December 2009 at Hiroshima University

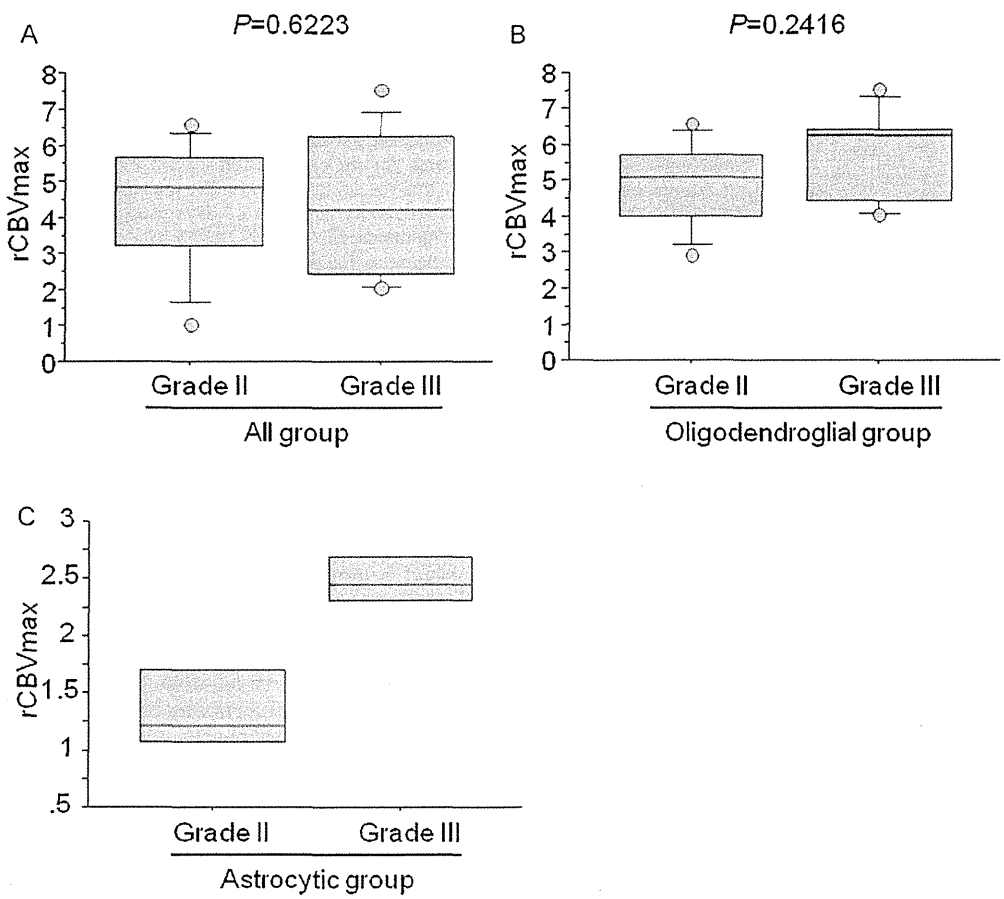

Fig. 2. (A) Box plots of rCBVmax values for grade II and III tumors in the astrocytic and oligodendroglial groups along with their respective standard deviation values. (B) Box plots of rCBVmax values for grade II and III tumors in the oligodendroglial group along with their respective standard deviation values.

Table 1
Patient demograhics, histologic diagnosis, and rCBVmax values.

Patient	Sex	Age	Histology	rCBVmax
Astrocytic group				
1	F	45	Diffuse astrocytoma	1.03
2	M	50	Difluse astrocytoma	1.86
3	M	51	Diffuse astrocytoma	1.21
4	M	42	Anaplastic astrocytoma	2.12
5	F	64	Anaplastic astrocytoma	2.85
6	M	44	Anaplastic astrocytoma	2.03
7	M	11	Anaplastic astrocytoma	2.25
Oligodendroglial group				
8	F	49	Oligoastrocytoma	5.60
9	M	58	Oligoastrocytoma	5.72
10	F	49	Oligoastrocytoma	4.02
11	M	48	Oligoastrocytoma	3.52
12	M	51	Oligoastrocytoma	4.63
13	F	34	Oligoastrocytoma	2.93
14	M	81	Anaplastic oligoastrocytoma	5.00
15	F	68	Anaplastic oligoastrocytoma	4.04
16	M	19	Anaplastic oligoastrocytoma	4.22
17	F	24	Anaplastic oligoastrocytoma	6.23
18	M	31	Oligodendroglioma	5.12
19	M	35	Oligodendroglioma	6.60
20	M	47	Oligodendroglioma	6.19
21	M	40	Oligodendroglioma	5.06
22	M	81	Anaplastic oligodendroglioma	6.46
23	F	48	Anaplastic oligodendroglioma	7.55
24	M	34	Anaplastic oligodendroglioma	6.23

Hospital. The study population comprised 16 males and 8 females; the median age was 46.0 ± 16.9 (11–81 years). Surgical specimens were histologically examined by an experienced neuropathologist (YT, 24 years of experience) blinded to clinical and MRI data. The histopathological assessment, carried out according to the criteria of the revised World Health Organization (WHO) classification, revealed 7 astrocytic tumors (3 grade II diffuse astrocytomas and 4 grade III anaplastic astrocytomas), 10 oligoastrocytic tumors (6 grade II oligoastrocytomas and 4 grade III anaplastic oligoastrocytomas), and 7 oligodendroglial tumors (4 grade II oligodendrogliomas and 3 grade III anaplastic oligodendrogliomas). For statistical purposes, the astrocytic tumors (7 patients) were designated as the astrocytic group, and the oligoastrocytic tumors and oligodendroglial tumors (17 patients) as the oligodendroglial group.

The study protocol was approved by the institutional review board of our institution; written informed consent from the patients was waived. To protect patient privacy, we removed all identifiers from our records upon the completion of our analyses.

2.2. Conventional MR imaging

MR examinations were performed using a 3 T system (Signa EXCITE 3.0 T; GE Medical Systems, Milwaukee, WI, USA) with a circularly polarized head coil. All patients underwent MRI studies that included at least unenhanced and contrast-enhanced transverse T1-weighted-, unenhanced transverse T2-weighted-, and unenhanced transverse fluid-attenuated inversion-recovery (FLAIR) images. The transverse T1-weighted spin-echo MR sequence was performed using the following parameters: repetition time ms/echo time ms, 400/17; field of view (FOV), 22 cm × 22 cm; matrix size, 288 (frequency), 192 (phase); section thickness, 6 mm; section gap, 1.0 mm; signal acquired, 2. The contrast-enhanced T1-weighted sequences were obtained after administering 0.1 mmol gadolinium compound per kg body weight. The transverse fast spin-echo T2-weighted sequence was performed using the following parameters: repetition time ms/echo time ms, 4800/100; FOV, 22 cm × 22 cm; matrix size, 512 × 320; echo train length, 18; section thickness, 6 mm; section gap, 1.0 mm; 2 signals. Transverse FLAIR images were acquired using fast and interleaved multi-section sequences with the following parameters: repetition time ms/echo time ms, 10,000/150; inversion time, 2400 ms; FOV, 22 cm × 22 cm; matrix size, 288 × 160; echo train length, 16; section thickness, 6 mm; section gap, 1.0 mm; 1 signal.

2.3. Perfusion imaging and region of interest analysis

PWI was obtained with a single-shot, gradient-echo-type echo-planar imaging (section thickness, 6 mm; gap, 1.0 mm; TR, 2000 ms; TE, 40 ms; FOV, 26 cm × 22 cm; matrix, 128 × 128; NEX, 1; slice, 15; phase, 40; acquisition time, 1 min 20 s). After the first 5 acquisitions, a bolus of gadolinium (0.1 mmol/kg) was injected with a mechanical injection pump (3 ml/s) through a 20-gauge intravenous catheter, followed by a 20-ml saline flush as previously reported [8]. The images were inspected for overall image quality and motion artifacts and were then transferred to a workstation for post-processing with a dedicated software package (Functool Performance, GE Medical Systems). On a voxel-by-voxel basis, the software calculated the curves of signal intensity changes over time, T_2^* relaxation rate (ΔR_2^*), the baseline to be subtracted from the ΔR_2^* curve, and area under the fitted ΔR_2^* curve. The ΔR_2^* was calculated using the equation: $\Delta R_2^* = -\ln(S_t/S_0)/\mathrm{TE}$, where S_t is the signal intensity at time t, S_0 is the precontrast signal intensity (excluding the first one or two images acquired while reaching the steady-state MR signal), and TE is the echo time. The baseline was estimated by calculating the average background intensity prior to onset and after completion of the transient signal intensity change. Color-coded rCBV maps were generated by the numerical integration of ΔR_2^* for the first-pass bolus through each pixel on the basis of kinetic principles for non-diffusible tracers.

For each slice, one region of interest (ROI) of 50 mm^2 was placed within the tumor on the area showing the most elevated CBV on color perfusion maps. Six more ROIs were positioned in the contralateral normal white matter. Margins of gliomas were delineated on T2-weighted and FLAIR images. To minimize confounding factors in relative CBV analysis, the size of the ROIs were kept constant for all tumors. Special attention was given to avoid placing ROIs over blood vessels—especially larger ones. The maximum CBV

values of all intra-tumoral ROIs, and the mean CBV of the contralateral ROIs were calculated. The rCBVmax values were then expressed as a ratio of the maximum rCBV value within the tumor to the mean CBV value in the contra-lateral normal appearing white matter. This approach has been demonstrated to provide the best inter- and intra-observer reproducibility [5]. Two authors (TS and FY, with 14 and 18 years of experience in brain MR imaging, respectively) who were blinded to the histological diagnosis, identified the ROIs after arriving at a consensus.

2.4. Statistical analysis

Data were analyzed using the SPSS (version 16.0) software package (SPSS Inc., Chicago, IL, USA). Multiple comparison tests, including the Tukey–Kramer test, were used for statistical comparison of the rCBVmax values between astrocytic, oligoastrocytic, and oligodendroglial tumors. Correlations between the subgroups of histology and patients characteristics (age, sex, and rCBVmax value) were calculated using Fisher's exact probability test. The Mann–Whitney test was used for statistical comparison of rCBVmax values between grade II and III tumors in all groups, as well as grade II and III tumors in the oligodendroglial group. A P value < 0.05 indicated a statistically significant difference.

3. Results

The demographics of the patient population, histologic diagnosis, and rCBVmax values are shown in Table 1. The average rCBVmax of astrocytic tumors (2.01 ± 0.68) was significantly lower than that of oligoastrocytic tumors (4.60 ± 1.05) and oligodendroglial tumors (6.17 ± 0.867; Fig. 1). Furthermore, the average rCBVmax of oligodendroglial tumors was significantly greater than that of the oligoastrocytic tumors. A threshold value of 3.0 allowed differentiation between the oligodendroglial and astrocytic groups at 100% sensitivity and 87.5% specificity with only one over-lapped patient (Fig. 1; Table 2).

No significant correlation was observed between the subgroups of histology, age (cut-off, mean age: 46 years), and sex (Table 2). No significant differences were observed in the average rCBVmax between grade II and III tumors in the two groups or grade II and III tumors in the oligodendroglial group (Fig. 2A and B). However, the rCBVmax values of anaplastic astrocytomas tended to be greater than those of diffuse astrocytomas (Fig. 2C). Representative images are shown in Figs. 3–5.

4. Discussion

Differentiating oligodendroglial tumors from astrocytic tumors is often difficult by anatomic MR imaging. This is because the MR images suffer from non-specificity and the inability to depict anything beyond morphologic aberration. However, with the addition of non-anatomic, physiology-based MR imaging methods such as perfusion MR imaging, more sophisticated tumor characterizations that can provide insight into underlying biological characteristics are now possible. Previous reports showed that most oligodendroglial tumors exhibit higher rCBVmax values than astrocytic tumors, irrespective of tumor grade [3]. Histopathologically, Schiffer et al. described the unique vascularity of oligodendrogliomas, in which an increased vascular density was observed in both low and high-grade oligodendrogliomas [9]. Subsequently, Lev et al. suggested that different perfusion patterns in astrocytic and oligodendroglial tumors are probably associated with the fine capillary network typically observed in oligodendrogliomas [3]. However, previous studies evaluated these tumors using 1.5 T MR imaging and found significant overlaps of the rCBV values between astrocytic and oligodendroglial tumors [2,3,10]. Our data demonstrated that the rCBVmax value obtained from 3 T MR PWI could differentiate the oligodendroglial group from the astrocytic group with less overlaps. This is the first reported study to clarify the role of 3 T MR PWI in the differentiation between astrocytic and oligodendroglial tumors. The cut-off ratio of 3.0 yielded 100% sensitivity and 87.5% specificity for the differentiation of the oligodendroglial group from the astrocytic group. We hypothesize that the difference between previous results and those of the current study are due to the advantages of using 3 T MR imaging.

DSC PWI benefits from the advantages of 3 T MR imaging [7,11]. The increased SNR and magnetic susceptibility of 3 T compared to those of 1.5 T results in images of brain tumors that are far more reliable [7]. Data can be obtained using smaller voxels (enhanced spatial resolution) at shorter time intervals (enhanced time resolution) by exploiting the increased SNR offered by 3 T MR systems. Furthermore, the frequent use of T_2* sequences in perfusion studies also offers some potential advantages. In particular, the increased susceptibility effect in addition to shorter relaxation times at 3 T results in increased sensitivity to transitory T_2* changes due to the bolus of contrast medium during capillary passage [6]. It has been suggested that these advantages allow the evaluation to be sensitive to the fine capillary network of oligodendroglial tumors and could lead to a clear differentiation between the oligodendroglial and astrocytic groups.

Differentiating oligodendroglial tumors from astrocytic tumors is important clinically because these two tumor types are well-defined, clinicopathological entities with distinct biological and prognostic characteristics [1]. Patients with oligodendroglial tumors are more likely to respond to chemotherapy and enjoy a longer progression-free survival than patients with astrocytic tumors of comparable malignancy grade [12]. However, neither clear diagnostic criteria nor reliable markers exist for oligodendroglioma—in part, this diagnosis rests on subjective criteria. The clinical need to distinguish oligodendroglial from astrocytic tumors appears to have resulted in a widening of the histological criteria for oligodendroglial tumors and an increase in the frequency of oligodendroglial tumors as well as a decrease in astrocytic tumors [13]. Consequently, the number of patients with astrocytic tumors in this study was low. Furthermore, the distinction between mixed oligoastrocytic tumors and oligodendroglial or astrocytic tumors is difficult and varies between different pathologists [13]. Some of the difficulties in the classification of oligoastrocytic tumors include the definition of oligodendroglial vs. astrocytic differentiation at the histological level and the minimal amount of oligodendroglial or astrocytic tumor cells required for the diagnosis of oligoastrocytic tumors [14]. The current data showed that the average rCBVmax of oligodendroglial tumors was significantly higher than that of oligoastrocytic tumors. Recently, Chang et al. reported the rCBV data of 134 patients with supratentorial gliomas. Their data showed the normalized median CBV values of 21 non-enhanced oligodendrogliomas (1.24, 0.83–2.27) to be higher than those of 13 non-enhanced oligoastrocytomas (0.95, 0.59–1.37) [15]. These results suggest that the more oligodendroglial component a tumor has, the higher is the rCBVmax value observed in the tumor. Therefore, the rCBVmax values obtained from 3 T MR PWI may also help to the postoperative histopathological diagnosis in the differentiation between oligoastrocytomas and oligodendrogliomas.

The current study found no significant difference in the average rCBVmax value between grade II and III tumors in the astrocytic and oligodendroglial groups. Several previous studies have suggested that rCBV measurement may improve the grading of gliomas [3,16–18]. However, Lev et al. and Arvinda et al. indicated that low-grade oligodendrogliomas show high rCBV foci and thus confound the reliability of rCBV values in distinguishing high-grade gliomas

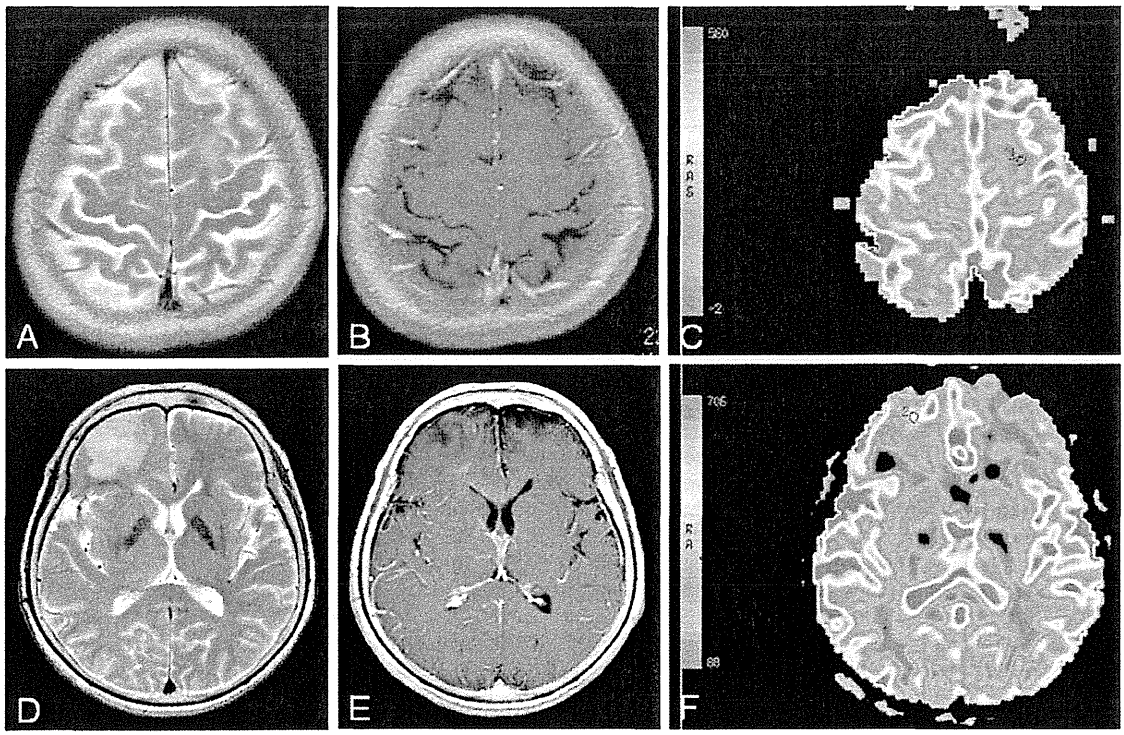

Fig. 3. (A–C) A representative case of a diffuse astrocytoma. (A) Axial transverse T2-weighted image shows a left frontal tumor. (B) Axial contrast-enhanced transverse T1-weighted image shows the tumor without enhancement. (C) The rCBV map shows that the rCBVmax value of the tumor is 1.03. (D–F) Representative case of an anaplastic astrocytoma. (D) Axial transverse T2-weighted image shows a right frontal tumor. (E) Axial contrast-enhanced transverse T1-weighted image shows the tumor with partial enhancement. (F) The rCBV map shows that the rCBVmax value of the tumor is 2.85.

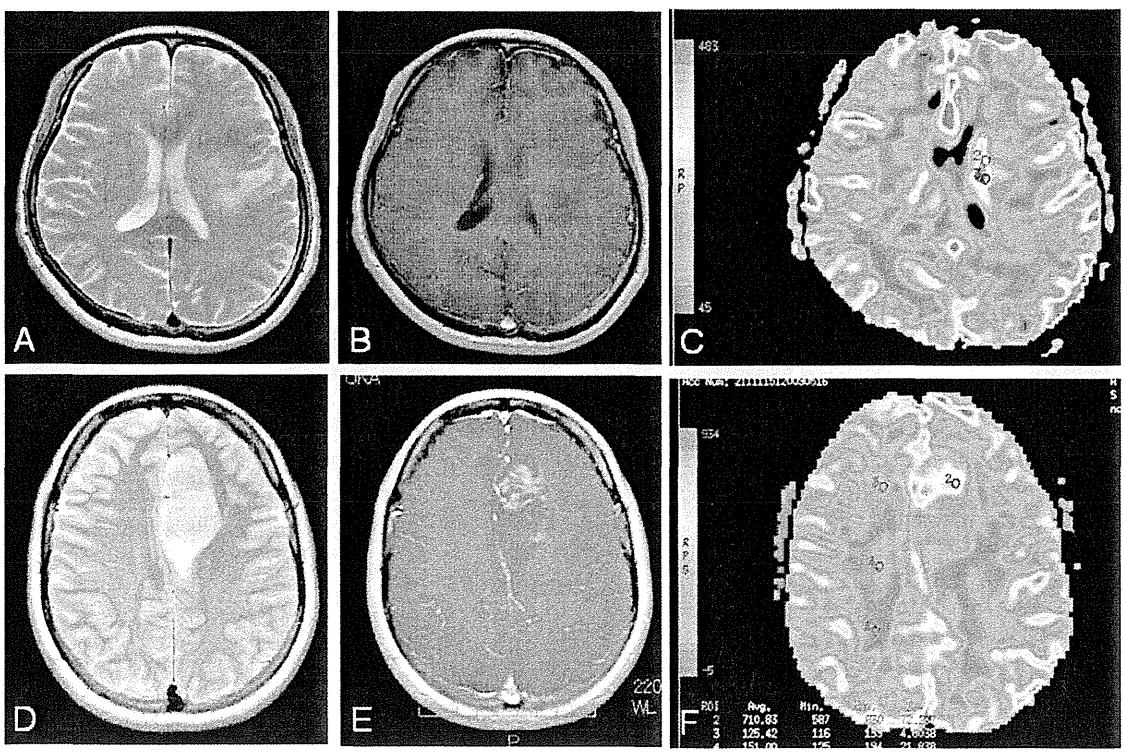

Fig. 4. (A–C) A representative case of an oligoastrocytoma. (A) Axial transverse T2-weighted image shows a left frontal tumor. (B) Axial contrast-enhanced transverse T1-weighted image shows the tumor with partial enhancement. (C) The rCBV map shows that the rCBVmax value of the tumor is 5.72. (D–F) A representative case of an anaplastic oligoastrocytoma. (D) Axial transverse T2-weighted image shows a left frontal tumor. (E) Axial contrast-enhanced transverse T1-weighted image shows the tumor with partial enhancement. (F) The rCBV map shows that the rCBVmax value of the tumor is 6.23.

Table 2
Subgroups of histology and patients characteristics.

	Subgroups of histology			*P* value
	Astrocytic group	Oligodendroglial group	Total	
Number of patients	7	17	24	
Age (mean)				0.6591
<46 years	4	7	11	
>46 years	3	10	13	>0.9999
Sex				
Male	5	11	16	
Female	2	6	8	
rCBVmax				0.0001*
<3.0	7	1	8	
>3.0	0	16	16	

Statistical analysis performed by Fisher's exact probability test.
* $P < 0.05$.

from low-grade ones [3,19]. Furthermore, the current study found no significant difference in the average rCBVmax between grade II and III tumors in the oligodendroglial group. Spampinato et al. analyzed the rCBV values of 22 patients with oligodendrogliomas or oligoastrocytomas and suggested that rCBV measurements are helpful in differentiating between low-grade and anaplastic oligodendroglial tumors [20]. However, their study included 5 patients with recurrent tumors after treatment (23%, 5/22 patients). Therefore, the inclusion of recurrent tumors in their study may be the cause of the differences between that study and the current one. The present series suggested that the grading of oligodendroglial tumors is difficult to make using rCBV assessments alone, due to their unique histological components. On the other hand, in the current study, the rCBVmax values of anaplastic astrocytomas tended to be higher than those of diffuse astrocytomas. Lev et al. also found a significant positive correlation between the astrocytic tumor grade and rCBV values [3]. Therefore, our and their results suggest that glioma grading based on rCBV measurement should be examined while excluding oligodendroglial tumors.

Our study has some limitations. First, the study population was rather small at 24 patients; larger prospective studies should be planned in order to achieve more definitive conclusions regarding the use of rCBVmax values for patient management. Second, there was no direct correlation between the focus of the rCBVmax value and the histopathological correlation. Further investigation aiming to directly correlate imaging with the histopathological findings, such as the tumor removal with stereotactic technique, will strengthen the validity of rCBVmax values using 3 T MR PWI as a noninvasive imaging marker of tumor subtype. Third, oligodendroglial tumors have exhibited relevant genetic profiling with

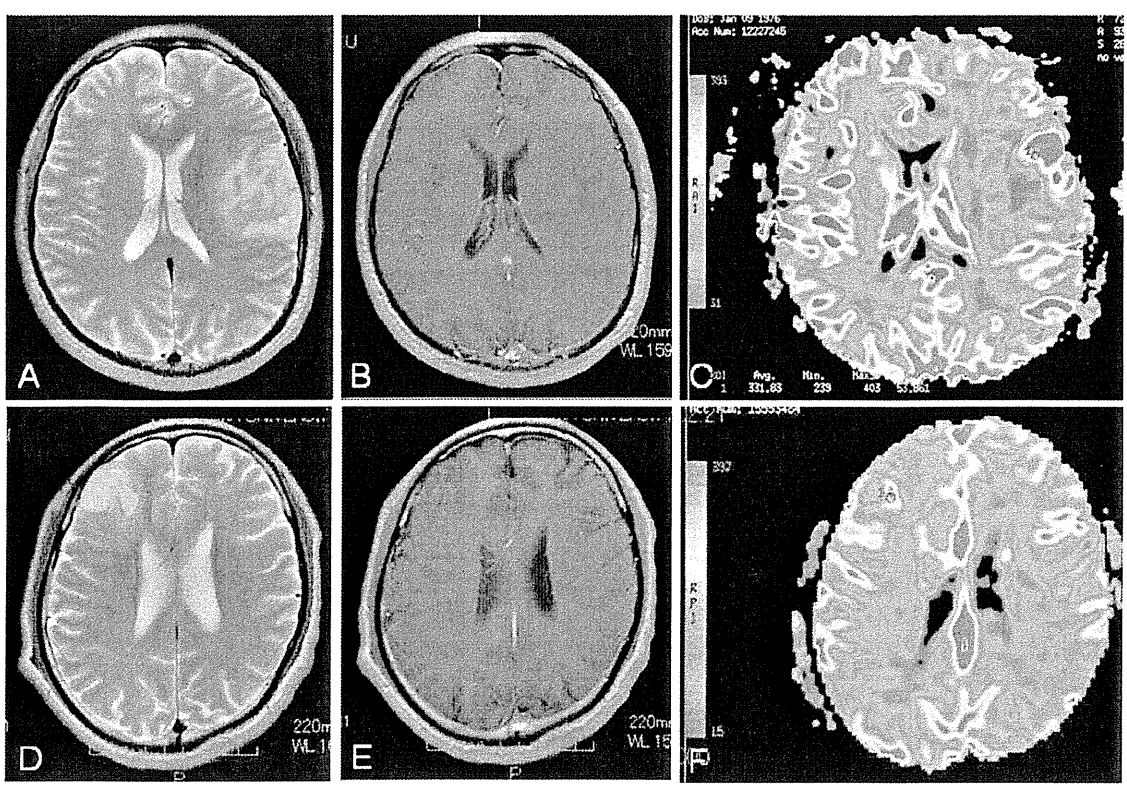

Fig. 5. (A–C) A representative case of an oligodendroglioma. (A) Axial transverse T2-weighted image shows a left frontal tumor. (B) Axial contrast-enhanced transverse T1-weighted image shows the tumor with faint partial enhancement. (C) The rCBV map shows that the rCBVmax value of the tumor is 5.12. (D–F) A representative case of an anaplastic oligodendroglioma. (D) Axial transverse T2-weighted image shows a right frontal tumor. (E) Axial contrast-enhanced transverse T1-weighted image shows the tumor without enhancement. (F) The rCBV map shows that the rCBVmax value of the tumor is 6.23.

1p/19q loss of heterozygosity. However, we did not analyze the relationship between our findings and the genetics of such tumors. In the future, further investigations aiming to correlate our findings with genetics are needed.

5. Conclusions

The present study is the first report to evaluate the role of 3 T MR PWI in differentiating between astrocytic and oligodendroglial tumors. The results showed that the rCBVmax values obtained from 3 T MR PWI may differentiate the oligodendroglial group from the astrocytic group with high sensitivity and specificity. Although only 3 T MR PWI could not clearly differentiate between these groups preoperatively, this approach may be useful as an adjunct to a post-operative histopathological diagnosis in patients presenting with gliomas.

Conflict of interest

The authors have no personal financial or institutional interest in any of the drugs, materials, or devices described in this article.

Acknowledgement

This study was supported in part by Grants-in-Aid for Scientific Research from the Ministry of Education, Culture, Sports, Science and Technology of Japan (grant no. 21791365).

References

[1] van den Bent M, Chinot OL, Cairncross JG. Recent developments in the molecular characterization and treatment of oligodendroglial tumors. Neuro Oncol 2003;5(2):128–38.
[2] Cha S, Tihan T, Crawford F, et al. Differentiation of low-grade oligodendrogliomas from low-grade astrocytomas by using quantitative blood-volume measurements derived from dynamic susceptibility contrast-enhanced MR imaging. AJNR Am J Neuroradiol 2005;26(2):266–73.
[3] Lev MH, Ozsunar Y, Henson JW, et al. Glial tumor grading and outcome prediction using dynamic spin-echo MR susceptibility mapping compared with conventional contrast-enhanced MR: confounding effect of elevated rCBV of oligodendrogliomas [corrected]. AJNR Am J Neuroradiol 2004;25(2):214–21.
[4] Maia Jr AC, Malheiros SM, da Rocha AJ, et al. MR cerebral blood volume maps correlated with vascular endothelial growth factor expression and tumor grade in nonenhancing gliomas. AJNR Am J Neuroradiol 2005;26(4):777–83.
[5] Wetzel SG, Cha S, Johnson G, et al. Relative cerebral blood volume measurements in intracranial mass lesions: interobserver and intraobserver reproducibility study. Radiology 2002;224(3):797–803.
[6] Frayne R, Goodyear BG, Dickhoff P, Lauzon ML, Sevick RJ. Magnetic resonance imaging at 3.0 Tesla: challenges and advantages in clinical neurological imaging. Invest Radiol 2003;38(7):385–402.
[7] Scarabino T, Giannatempo GM, Popolizio T, et al. 3.0-T functional brain imaging: a 5-year experience. Radiol Med 2007;112(1):97–112.
[8] Manka C, Traber F, Gieseke J, Schild HH, Kuhl CK. Three-dimensional dynamic susceptibility-weighted perfusion MR imaging at 3.0 T: feasibility and contrast agent dose. Radiology 2005;234(3):869–77.
[9] Schiffer D, Bosone I, Dutto A, Di Vito N, Chio A. The prognostic role of vessel productive changes and vessel density in oligodendroglioma. J Neurooncol 1999;44(2):99–107.
[10] Bisdas S, Kirkpatrick M, Giglio P, Welsh C, Spampinato MV, Rumboldt Z. Cerebral blood volume measurements by perfusion-weighted MR imaging in gliomas: ready for prime time in predicting short-term outcome and recurrent disease? AJNR Am J Neuroradiol 2009;30(4):681–8.
[11] Di Costanzo A, Scarabino T, Trojsi F, et al. Multiparametric 3 T MR approach to the assessment of cerebral gliomas: tumor extent and malignancy. Neuroradiology 2006;48(9):622–31.
[12] Burger PC. What is an oligodendroglioma? Brain Pathol 2002;12(2):257–9.
[13] Louis DN, Ohgaki H, Wiestler OD, et al. The 2007 WHO classification of tumours of the central nervous system. Acta Neuropathol 2007;114(2):97–109.
[14] Jeuken JW, von Deimling A, Wesseling P. Molecular pathogenesis of oligodendroglial tumors. J Neurooncol 2004;70(2):161–81.
[15] Chang SM, Nelson S, Vandenberg S, et al. Integration of preoperative anatomic and metabolic physiologic imaging of newly diagnosed glioma. J Neurooncol 2009;92(3):401–15.
[16] Cha S, Knopp EA, Johnson G, Wetzel SG, Litt AW, Zagzag D. Intracranial mass lesions: dynamic contrast-enhanced susceptibility-weighted echo-planar perfusion MR imaging. Radiology 2002;223(1):11–29.
[17] Preul C, Kuhn B, Lang EW, Mehdorn HM, Heller M, Link J. Differentiation of cerebral tumors using multi-section echo planar MR perfusion imaging. Eur J Radiol 2003;48(3):244–51.
[18] Law M, Yang S, Wang H, et al. Glioma grading: sensitivity, specificity, and predictive values of perfusion MR imaging and proton MR spectroscopic imaging compared with conventional MR imaging. AJNR Am J Neuroradiol 2003;24(10):1989–98.
[19] Arvinda HR, Kesavadas C, Sarma PS, et al. Glioma grading: sensitivity, specificity, positive and negative predictive values of diffusion and perfusion imaging. J Neurooncol 2009;94(1):87–96.
[20] Spampinato MV, Smith JK, Kwock L, et al. Cerebral blood volume measurements and proton MR spectroscopy in grading of oligodendroglial tumors. AJR Am J Roentgenol 2007;188(1):204–12.

European Journal of Radiology 81 (2012) 1863–1869

Contents lists available at ScienceDirect

European Journal of Radiology

journal homepage: www.elsevier.com/locate/ejrad

Role of perfusion-weighted imaging at 3 T in the histopathological differentiation between astrocytic and oligodendroglial tumors

Taiichi Saito[a,*], Fumiyuki Yamasaki[a], Yoshinori Kajiwara[a], Nobukazu Abe[b,1], Yuji Akiyama[b], Takako Kakuda[b], Yukio Takeshima[c,2], Kazuhiko Sugiyama[a], Yoshikazu Okada[d,3], Kaoru Kurisu[a]

[a] Department of Neurosurgery, Hiroshima University, 1-2-3 Kasumi, Minami-ku, Hiroshima 734-8551, Japan
[b] Department of Clinical Radiology, Hiroshima University, 1-2-3 Kasumi, Minami-ku, Hiroshima 734-8551, Japan
[c] Department of Pathology, Hiroshima University, 1-2-3 Kasumi, Minami-ku, Hiroshima 734-8551, Japan
[d] Department of Neurosurgery, Tokyo Women's Medical University, 8-1 Kawada, Shinjuku-ku, Tokyo 162-8666, Japan

ARTICLE INFO

Article history:
Received 4 January 2011
Accepted 5 April 2011

Keywords:
Perfusion imaging
Magnetic resonance imaging
Oligodendroglioma
Astrocytoma
Glioma

ABSTRACT

Objective: The differentiation of oligodendroglial tumors from astrocytic tumors is important clinically, because oligodendroglial tumors are more chemosensitive than astrocytic tumors. This study was designed to clarify the usefulness of 3 T MR perfusion imaging (PWI) in the histopathological differentiation between astrocytic and oligodendroglial tumors. This is because there is a growing interest in the diagnostic performance of 3 T MR imaging, which has the advantages of a higher signal-to-noise ratio (SNR) and greater spatial and temporal resolution.

Materials and methods: This study retrospectively included 24 consecutive patients with supratentorial, WHO grade II and III astrocytic and oligodendroglial tumors (7 astrocytic, 10 oligoastrocytic, and 7 oligodendroglial tumors) that were newly diagnosed and resected between November 2006 and December 2009 at Hiroshima University Hospital. These patients underwent dynamic susceptibility contrast-enhanced (DSC) PWI relative cerebral blood volume (rCBV) measurements before treatment. Astrocytic tumors were designated as the astrocytic group, and oligoastrocytic and oligodendroglial tumors as the oligodendroglial group. The regions of interest with the maximum rCBV values within the tumors were normalized relative to the contra-lateral white matter (rCBVmax).

Results: The average rCBVmax of astrocytic tumors (2.01 ± 0.68) was significantly lower than that of the oligoastrocytic (4.60 ± 1.05) and oligodendroglial tumors (6.17 ± 0.867) ($P < 0.0001$). A cut-off value of 3.0 allowed to differentiate the oligodendroglial group from the astrocytic group at 100% sensitivity and 87.5% specificity.

Conclusion: The rCBVmax values obtained from 3 T MR PWI may be useful as an adjunct to the postoperative histopathological diagnosis of glioma patients.

1. Introduction

The differentiation of gliomas containing oligodendroglial components from astrocytic tumors is important clinically, because oligodendroglial and oligoastrocytic tumors are more chemosensitive than astrocytic tumors [1]. However, the differentiation of these tumors is sometimes difficult, because of the ambiguous criteria. Although a histopathological evaluation remains the reference standard for the histological subtyping of gliomas, this method is limited by issues such as subjective criteria, heterogeneity within tumors, and tissue sampling errors. Attempts have been made to enhance the prognostic information obtained by the histological classification of gliomas. Therefore, additional supportive information is required histopathological classification. Recently, dynamic susceptibility contrast-enhanced (DSC) MR perfusion imaging (PWI) has been used as part of a combined approach with histopathology in order to help to accurately subtype brain tumors [2,3].

There is evidence that MR PWI may be a sensitive marker of the microvascular density in gliomas. Relative cerebral blood volume (rCBV) measurements are closely correlated with angio-

* Corresponding author. Tel.: +81 82 257 5227; fax: +81 82 257 5229.
E-mail addresses: t-saitou@qc4.so-net.ne.jp (T. Saito), fyama@hiroshima-u.ac.jp (F. Yamasaki), kaji@hiroshima-u.ac.jp (Y. Kajiwara), abebe@hiroshima-u.ac.jp (N. Abe), uakiyama@hiroshima-u.ac.jp (Y. Akiyama), taka4121@hiroshima-u.ac.jp (T. Kakuda), ykotake@hiroshima-u.ac.jp (Y. Takeshima), brain@hiroshima-u.ac.jp (K. Sugiyama), yokada@nij.twmu.ac.jp (Y. Okada), kuka422@hiroshima-u.ac.jp (K. Kurisu).
[1] Tel: +81 82 257 5257.
[2] Tel: +81 82 257 5152; fax: +81 82 257 5154.
[3] Tel: +81 3 3353 8111; fax: +81 3 5269 7438.

0720-048X/$ – see front matter © 2011 Elsevier Ireland Ltd. All rights reserved.
doi:10.1016/j.ejrad.2011.04.009

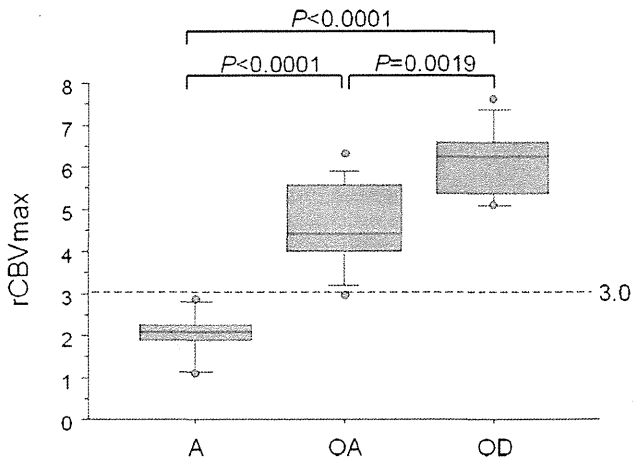

Fig. 1. Box plots of rCBVmax values for astrocytic tumors, oligoastrocytic tumors, and oligodendroglial tumors along with their respective standard deviation values. The cut-off line of 3.0 yields 100% sensitivity and 87.5% specificity for differentiating the oligodendroglial group (oligoastrocytic tumors and oligodendroglial tumors) from the astrocytic group. A, astrocytic tumors; OA, oligoastrocytic tumors; OD, oligodendroglial tumors.

graphic and histologic markers of tumor vascularity [4]. Perfusion image-based brain tumor characterization is currently performed by assessing the maximum ratio between an rCBV area within the glioma and the unaffected contralateral rCBV value (rCBVmax) [5]. Oligodendrogliomas often have an attenuated network of branching capillaries resembling a chicken wire pattern. Most oligodendroglial tumors (oligodendrogliomas and oligoastrocytomas) exhibit higher rCBVmax values than astrocytic tumors [3].

Some reports have demonstrated the usefulness of PWI in the assessment of hemodynamics in gliomas and differentiation of oligodendroglial tumors from astrocytic tumors [3]. However, these reports used 1.5 T MR imaging, and significant overlaps of rCBVmax values were observed between astrocytic and oligodendroglial tumors. Recently, with the integration of 3 T imaging into clinical practice, there is a growing interest in the diagnostic performance of 3 T MR imaging techniques with respect to the established magnetic field strength of 1.5 T [6,7]. MR performed at higher magnetic field strengths has the advantages of higher signal-to-noise ratio (SNR) and magnetic susceptibility; this results in improved spatial and temporal resolution [6,7]. Therefore, these advantages may help improve the accuracy of differential diagnoses of gliomas. Therefore, this study was designed to characterize the hemodynamics within gliomas by using 3 T MR PWI and clarify whether this approach help the postoperative histopathological diagnosis in the differentiation between astrocytic and oligodendroglial tumors.

2. Materials and methods

2.1. Patients and histological diagnosis

This study retrospectively included 24 consecutive patients with supratentorial, WHO grade II and III astrocytic and oligodendroglial tumors that were newly diagnosed and resected between November 2006 and December 2009 at Hiroshima University

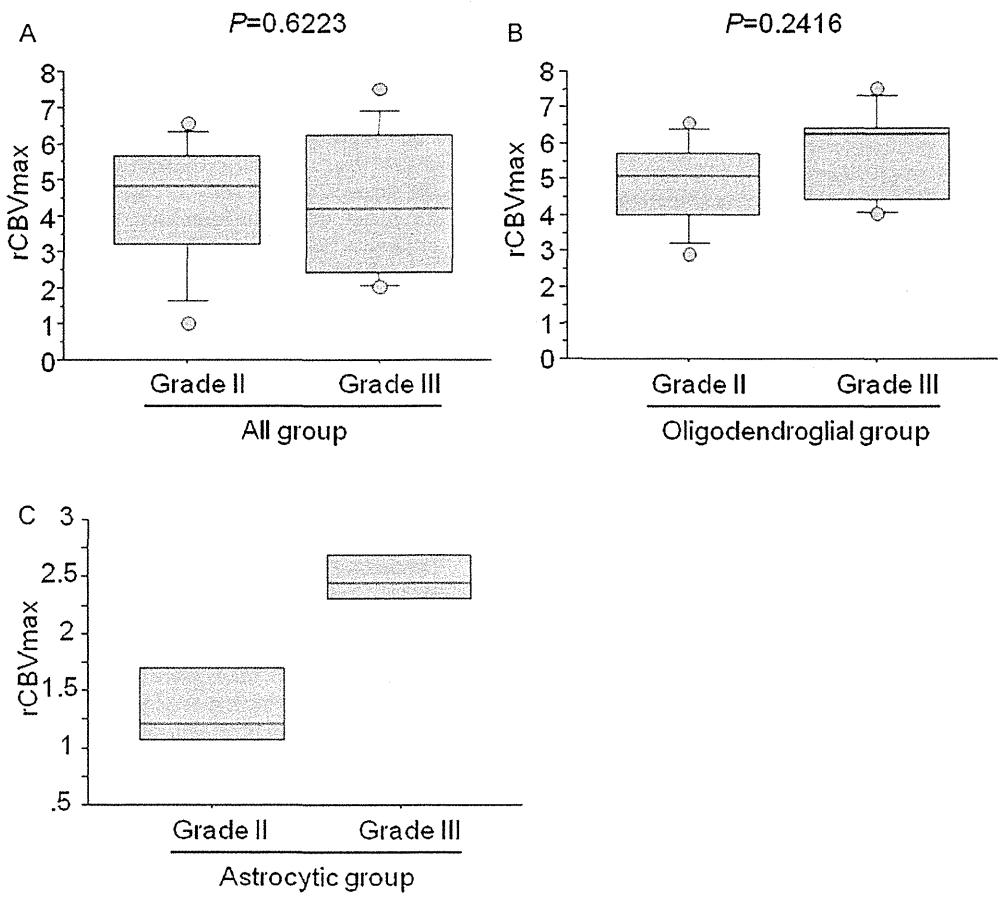

Fig. 2. (A) Box plots of rCBVmax values for grade II and III tumors in the astrocytic and oligodendroglial groups along with their respective standard deviation values. (B) Box plots of rCBVmax values for grade II and III tumors in the oligodendroglial group along with their respective standard deviation values.

Table 1
Patient demograhics, histologic diagnosis, and rCBVmax values.

Patient	Sex	Age	Histology	rCBVmax
Astrocytic group				
1	F	45	Diffuse astrocytoma	1.03
2	M	50	Difluse astrocytoma	1.86
3	M	51	Diffuse astrocytoma	1.21
4	M	42	Anaplastic astrocytoma	2.12
5	F	64	Anaplastic astrocytoma	2.85
6	M	44	Anaplastic astrocytoma	2.03
7	M	11	Anaplastic astrocytoma	2.25
Oligodendroglial group				
8	F	49	Oligoastrocytoma	5.60
9	M	58	Oligoastrocytoma	5.72
10	F	49	Oligoastrocytoma	4.02
11	M	48	Oligoastrocytoma	3.52
12	M	51	Oligoastrocytoma	4.63
13	F	34	Oligoastrocytoma	2.93
14	M	81	Anaplastic oligoastrocytoma	5.00
15	F	68	Anaplastic oligoastrocytoma	4.04
16	M	19	Anaplastic oligoastrocytoma	4.22
17	F	24	Anaplastic oligoastrocytoma	6.23
18	M	31	Oligodendroglioma	5.12
19	M	35	Oligodendroglioma	6.60
20	M	47	Oligodendroglioma	6.19
21	M	40	Oligodendroglioma	5.06
22	M	81	Anaplastic oligodendroglioma	6.46
23	F	48	Anaplastic oligodendroglioma	7.55
24	M	34	Anaplastic oligodendroglioma	6.23

Hospital. The study population comprised 16 males and 8 females; the median age was 46.0 ± 16.9 (11–81 years). Surgical specimens were histologically examined by an experienced neuropathologist (YT, 24 years of experience) blinded to clinical and MRI data. The histopathological assessment, carried out according to the criteria of the revised World Health Organization (WHO) classification, revealed 7 astrocytic tumors (3 grade II diffuse astrocytomas and 4 grade III anaplastic astrocytomas), 10 oligoastrocytic tumors (6 grade II oligoastrocytomas and 4 grade III anaplastic oligoastrocytomas), and 7 oligodendroglial tumors (4 grade II oligodendrogliomas and 3 grade III anaplastic oligodendrogliomas). For statistical purposes, the astrocytic tumors (7 patients) were designated as the astrocytic group, and the oligoastrocytic tumors and oligodendroglial tumors (17 patients) as the oligodendroglial group.

The study protocol was approved by the institutional review board of our institution; written informed consent from the patients was waived. To protect patient privacy, we removed all identifiers from our records upon the completion of our analyses.

2.2. Conventional MR imaging

MR examinations were performed using a 3 T system (Signa EXCITE 3.0 T; GE Medical Systems, Milwaukee, WI, USA) with a circularly polarized head coil. All patients underwent MRI studies that included at least unenhanced and contrast-enhanced transverse T1-weighted-, unenhanced transverse T2-weighted-, and unenhanced transverse fluid-attenuated inversion-recovery (FLAIR) images. The transverse T1-weighted spin-echo MR sequence was performed using the following parameters: repetition time ms/echo time ms, 400/17; field of view (FOV), 22 cm × 22 cm; matrix size, 288 (frequency), 192 (phase); section thickness, 6 mm; section gap, 1.0 mm; signal acquired, 2. The contrast-enhanced T1-weighted sequences were obtained after administering 0.1 mmol gadolinium compound per kg body weight. The transverse fast spin-echo T2-weighted sequence was performed using the following parameters: repetition time ms/echo time ms, 4800/100; FOV, 22 cm × 22 cm; matrix size, 512 × 320; echo train length, 18; section thickness, 6 mm; section gap, 1.0 mm; 2 signals. Transverse FLAIR images were acquired using fast and interleaved multi-section sequences with the following parameters: repetition time ms/echo time ms, 10,000/150; inversion time, 2400 ms; FOV, 22 cm × 22 cm; matrix size, 288 × 160; echo train length, 16; section thickness, 6 mm; section gap, 1.0 mm; 1 signal.

2.3. Perfusion imaging and region of interest analysis

PWI was obtained with a single-shot, gradient-echo-type echo-planar imaging (section thickness, 6 mm; gap, 1.0 mm; TR, 2000 ms; TE, 40 ms; FOV, 26 cm × 22 cm; matrix, 128 × 128; NEX, 1; slice, 15; phase, 40; acquisition time, 1 min 20 s). After the first 5 acquisitions, a bolus of gadolinium (0.1 mmol/kg) was injected with a mechanical injection pump (3 ml/s) through a 20-gauge intravenous catheter, followed by a 20-ml saline flush as previously reported [8]. The images were inspected for overall image quality and motion artifacts and were then transferred to a workstation for post-processing with a dedicated software package (Functool Performance, GE Medical Systems). On a voxel-by-voxel basis, the software calculated the curves of signal intensity changes over time, T_2^* relaxation rate (ΔR_2^*), the baseline to be subtracted from the ΔR_2^* curve, and area under the fitted ΔR_2^* curve. The ΔR_2^* was calculated using the equation: $\Delta R_2^* = -\ln(S_t/S_0)/\mathrm{TE}$, where S_t is the signal intensity at time t, S_0 is the precontrast signal intensity (excluding the first one or two images acquired while reaching the steady-state MR signal), and TE is the echo time. The baseline was estimated by calculating the average background intensity prior to onset and after completion of the transient signal intensity change. Color-coded rCBV maps were generated by the numerical integration of ΔR_2^* for the first-pass bolus through each pixel on the basis of kinetic principles for non-diffusible tracers.

For each slice, one region of interest (ROI) of 50 mm^2 was placed within the tumor on the area showing the most elevated CBV on color perfusion maps. Six more ROIs were positioned in the contralateral normal white matter. Margins of gliomas were delineated on T2-weighted and FLAIR images. To minimize confounding factors in relative CBV analysis, the size of the ROIs were kept constant for all tumors. Special attention was given to avoid placing ROIs over blood vessels—especially larger ones. The maximum CBV

values of all intra-tumoral ROIs, and the mean CBV of the contra-lateral ROIs were calculated. The rCBVmax values were then expressed as a ratio of the maximum rCBV value within the tumor to the mean CBV value in the contra-lateral normal appearing white matter. This approach has been demonstrated to provide the best inter- and intra-observer reproducibility [5]. Two authors (TS and FY, with 14 and 18 years of experience in brain MR imaging, respectively) who were blinded to the histological diagnosis, identified the ROIs after arriving at a consensus.

2.4. Statistical analysis

Data were analyzed using the SPSS (version 16.0) software package (SPSS Inc., Chicago, IL, USA). Multiple comparison tests, including the Tukey–Kramer test, were used for statistical comparison of the rCBVmax values between astrocytic, oligoastrocytic, and oligodendroglial tumors. Correlations between the subgroups of histology and patients characteristics (age, sex, and rCBVmax value) were calculated using Fisher's exact probability test. The Mann–Whitney test was used for statistical comparison of rCBVmax values between grade II and III tumors in all groups, as well as grade II and III tumors in the oligodendroglial group. A P value < 0.05 indicated a statistically significant difference.

3. Results

The demographics of the patient population, histologic diagnosis, and rCBVmax values are shown in Table 1. The average rCBVmax of astrocytic tumors (2.01 ± 0.68) was significantly lower than that of oligoastrocytic tumors (4.60 ± 1.05) and oligodendroglial tumors (6.17 ± 0.867; Fig. 1). Furthermore, the average rCBVmax of oligodendroglial tumors was significantly greater than that of the oligoastrocytic tumors. A threshold value of 3.0 allowed differentiation between the oligodendroglial and astrocytic groups at 100% sensitivity and 87.5% specificity with only one over-lapped patient (Fig. 1; Table 2).

No significant correlation was observed between the subgroups of histology, age (cut-off, mean age: 46 years), and sex (Table 2). No significant differences were observed in the average rCBVmax between grade II and III tumors in the two groups or grade II and III tumors in the oligodendroglial group (Fig. 2A and B). However, the rCBVmax values of anaplastic astrocytomas tended to be greater than those of diffuse astrocytomas (Fig. 2C). Representative images are shown in Figs. 3–5.

4. Discussion

Differentiating oligodendroglial tumors from astrocytic tumors is often difficult by anatomic MR imaging. This is because the MR images suffer from non-specificity and the inability to depict anything beyond morphologic aberration. However, with the addition of non-anatomic, physiology-based MR imaging methods such as perfusion MR imaging, more sophisticated tumor characterizations that can provide insight into underlying biological characteristics are now possible. Previous reports showed that most oligodendroglial tumors exhibit higher rCBVmax values than astrocytic tumors, irrespective of tumor grade [3]. Histopathologically, Schiffer et al. described the unique vascularity of oligodendrogliomas, in which an increased vascular density was observed in both low and high-grade oligodendrogliomas [9]. Subsequently, Lev et al. suggested that different perfusion patterns in astrocytic and oligodendroglial tumors are probably associated with the fine capillary network typically observed in oligodendrogliomas [3]. However, previous studies evaluated these tumors using 1.5 T MR imaging and found significant overlaps of the rCBV values between astrocytic and oligodendroglial tumors [2,3,10]. Our data demonstrated that the rCBVmax value obtained from 3 T MR PWI could differentiate the oligodendroglial group from the astrocytic group with less overlaps. This is the first reported study to clarify the role of 3 T MR PWI in the differentiation between astrocytic and oligodendroglial tumors. The cut-off ratio of 3.0 yielded 100% sensitivity and 87.5% specificity for the differentiation of the oligodendroglial group from the astrocytic group. We hypothesize that the difference between previous results and those of the current study are due to the advantages of using 3 T MR imaging.

DSC PWI benefits from the advantages of 3 T MR imaging [7,11]. The increased SNR and magnetic susceptibility of 3 T compared to those of 1.5 T results in images of brain tumors that are far more reliable [7]. Data can be obtained using smaller voxels (enhanced spatial resolution) at shorter time intervals (enhanced time resolution) by exploiting the increased SNR offered by 3 T MR systems. Furthermore, the frequent use of T_2* sequences in perfusion studies also offers some potential advantages. In particular, the increased susceptibility effect in addition to shorter relaxation times at 3 T results in increased sensitivity to transitory T_2* changes due to the bolus of contrast medium during capillary passage [6]. It has been suggested that these advantages allow the evaluation to be sensitive to the fine capillary network of oligodendroglial tumors and could lead to a clear differentiation between the oligodendroglial and astrocytic groups.

Differentiating oligodendroglial tumors from astrocytic tumors is important clinically because these two tumor types are well-defined, clinicopathological entities with distinct biological and prognostic characteristics [1]. Patients with oligodendroglial tumors are more likely to respond to chemotherapy and enjoy a longer progression-free survival than patients with astrocytic tumors of comparable malignancy grade [12]. However, neither clear diagnostic criteria nor reliable markers exist for oligodendroglioma—in part, this diagnosis rests on subjective criteria. The clinical need to distinguish oligodendroglial from astrocytic tumors appears to have resulted in a widening of the histological criteria for oligodendroglial tumors and an increase in the frequency of oligodendroglial tumors as well as a decrease in astrocytic tumors [13]. Consequently, the number of patients with astrocytic tumors in this study was low. Furthermore, the distinction between mixed oligoastrocytic tumors and oligodendroglial or astrocytic tumors is difficult and varies between different pathologists [13]. Some of the difficulties in the classification of oligoastrocytic tumors include the definition of oligodendroglial vs. astrocytic differentiation at the histological level and the minimal amount of oligodendroglial or astrocytic tumor cells required for the diagnosis of oligoastrocytic tumors [14]. The current data showed that the average rCBVmax of oligodendroglial tumors was significantly higher than that of oligoastrocytic tumors. Recently, Chang et al. reported the rCBV data of 134 patients with supratentorial gliomas. Their data showed the normalized median CBV values of 21 non-enhanced oligodendrogliomas (1.24, 0.83–2.27) to be higher than those of 13 non-enhanced oligoastrocytomas (0.95, 0.59–1.37) [15]. These results suggest that the more oligodendroglial component a tumor has, the higher is the rCBVmax value observed in the tumor. Therefore, the rCBVmax values obtained from 3 T MR PWI may also help to the postoperative histopathological diagnosis in the differentiation between oligoastrocytomas and oligodendrogliomas.

The current study found no significant difference in the average rCBVmax value between grade II and III tumors in the astrocytic and oligodendroglial groups. Several previous studies have suggested that rCBV measurement may improve the grading of gliomas [3,16–18]. However, Lev et al. and Arvinda et al. indicated that low-grade oligodendrogliomas show high rCBV foci and thus confound the reliability of rCBV values in distinguishing high-grade gliomas

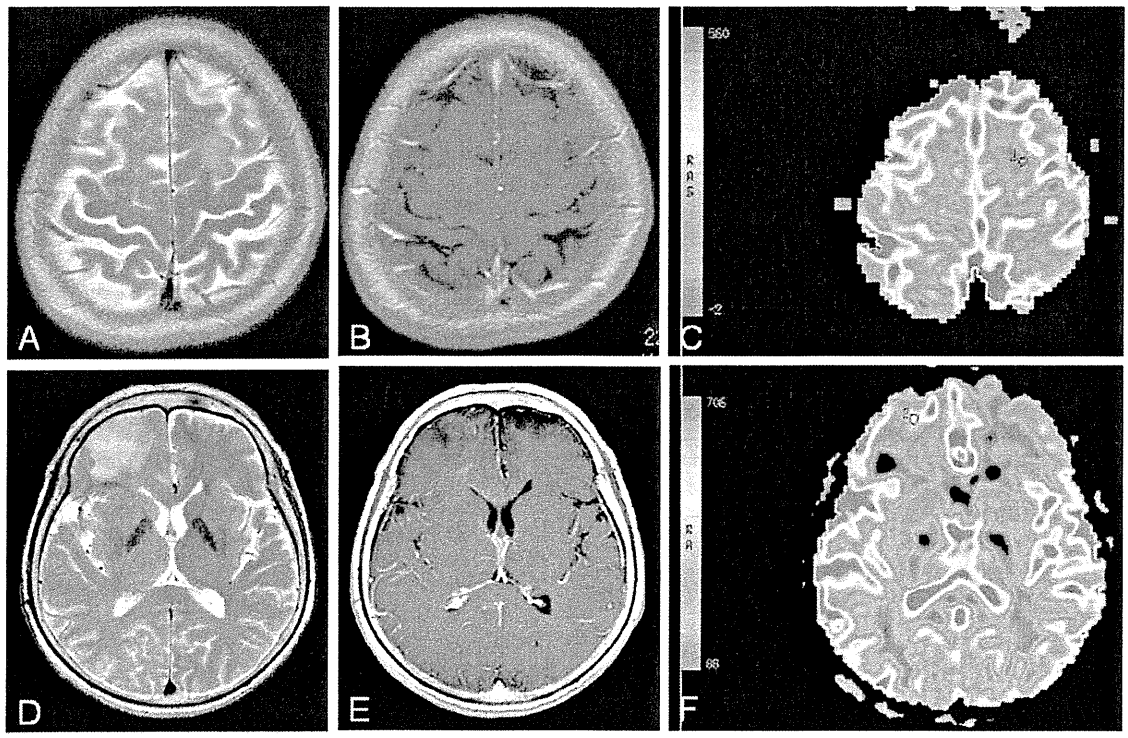

Fig. 3. (A–C) A representative case of a diffuse astrocytoma. (A) Axial transverse T2-weighted image shows a left frontal tumor. (B) Axial contrast-enhanced transverse T1-weighted image shows the tumor without enhancement. (C) The rCBV map shows that the rCBVmax value of the tumor is 1.03. (D–F) Representative case of an anaplastic astrocytoma. (D) Axial transverse T2-weighted image shows a right frontal tumor. (E) Axial contrast-enhanced transverse T1-weighted image shows the tumor with partial enhancement. (F) The rCBV map shows that the rCBVmax value of the tumor is 2.85.

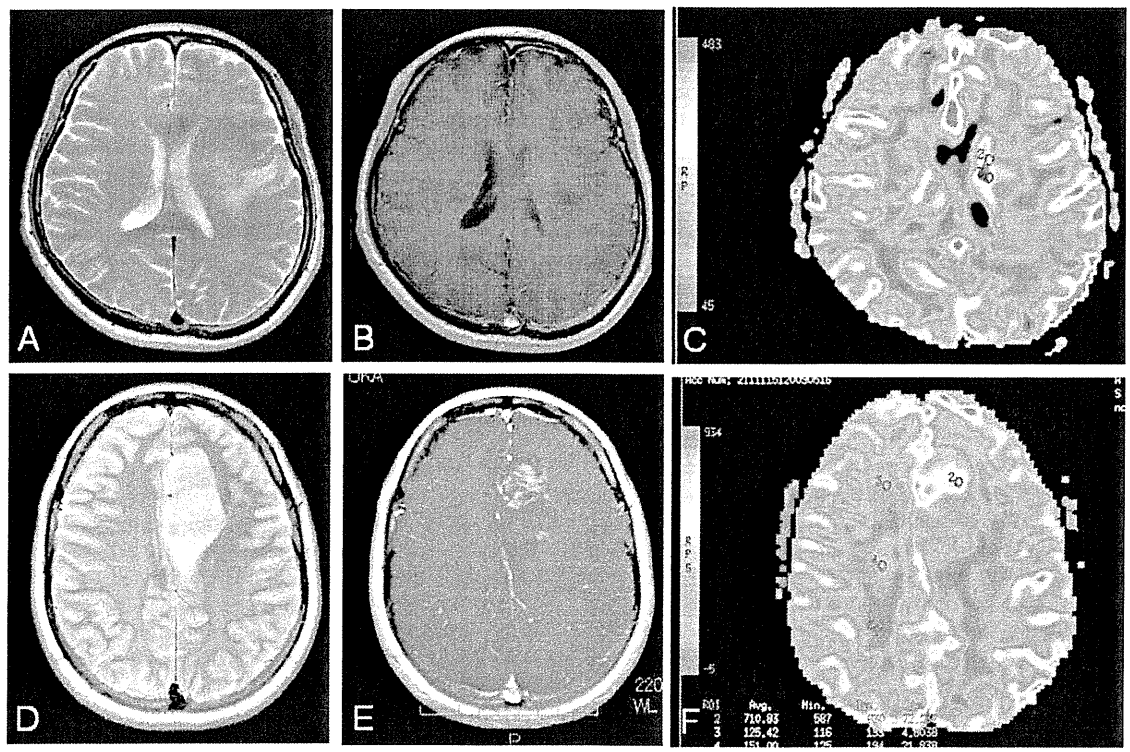

Fig. 4. (A–C) A representative case of an oligoastrocytoma. (A) Axial transverse T2-weighted image shows a left frontal tumor. (B) Axial contrast-enhanced transverse T1-weighted image shows the tumor with partial enhancement. (C) The rCBV map shows that the rCBVmax value of the tumor is 5.72. (D–F) A representative case of an anaplastic oligoastrocytoma. (D) Axial transverse T2-weighted image shows a left frontal tumor. (E) Axial contrast-enhanced transverse T1-weighted image shows the tumor with partial enhancement. (F) The rCBV map shows that the rCBVmax value of the tumor is 6.23.

Table 2
Subgroups of histology and patients characteristics.

	Subgroups of histology			*P* value
	Astrocytic group	Oligodendroglial group	Total	
Number of patients	7	17	24	
Age (mean)				0.6591
<46 years	4	7	11	
>46 years	3	10	13	>0.9999
Sex				
Male	5	11	16	
Female	2	6	8	
rCBVmax				0.0001*
<3.0	7	1	8	
>3.0	0	16	16	

Statistical analysis performed by Fisher's exact probability test.
* $P < 0.05$.

from low-grade ones [3,19]. Furthermore, the current study found no significant difference in the average rCBVmax between grade II and III tumors in the oligodendroglial group. Spampinato et al. analyzed the rCBV values of 22 patients with oligodendrogliomas or oligoastrocytomas and suggested that rCBV measurements are helpful in differentiating between low-grade and anaplastic oligodendroglial tumors [20]. However, their study included 5 patients with recurrent tumors after treatment (23%, 5/22 patients). Therefore, the inclusion of recurrent tumors in their study may be the cause of the differences between that study and the current one. The present series suggested that the grading of oligodendroglial tumors is difficult to make using rCBV assessments alone, due to their unique histological components. On the other hand, in the current study, the rCBVmax values of anaplastic astrocytomas tended to be higher than those of diffuse astrocytomas. Lev et al. also found a significant positive correlation between the astrocytic tumor grade and rCBV values [3]. Therefore, our and their results suggest that glioma grading based on rCBV measurement should be examined while excluding oligodendroglial tumors.

Our study has some limitations. First, the study population was rather small at 24 patients; larger prospective studies should be planned in order to achieve more definitive conclusions regarding the use of rCBVmax values for patient management. Second, there was no direct correlation between the focus of the rCBVmax value and the histopathological correlation. Further investigation aiming to directly correlate imaging with the histopathological findings, such as the tumor removal with stereotactic technique, will strengthen the validity of rCBVmax values using 3 T MR PWI as a noninvasive imaging marker of tumor subtype. Third, oligodendroglial tumors have exhibited relevant genetic profiling with

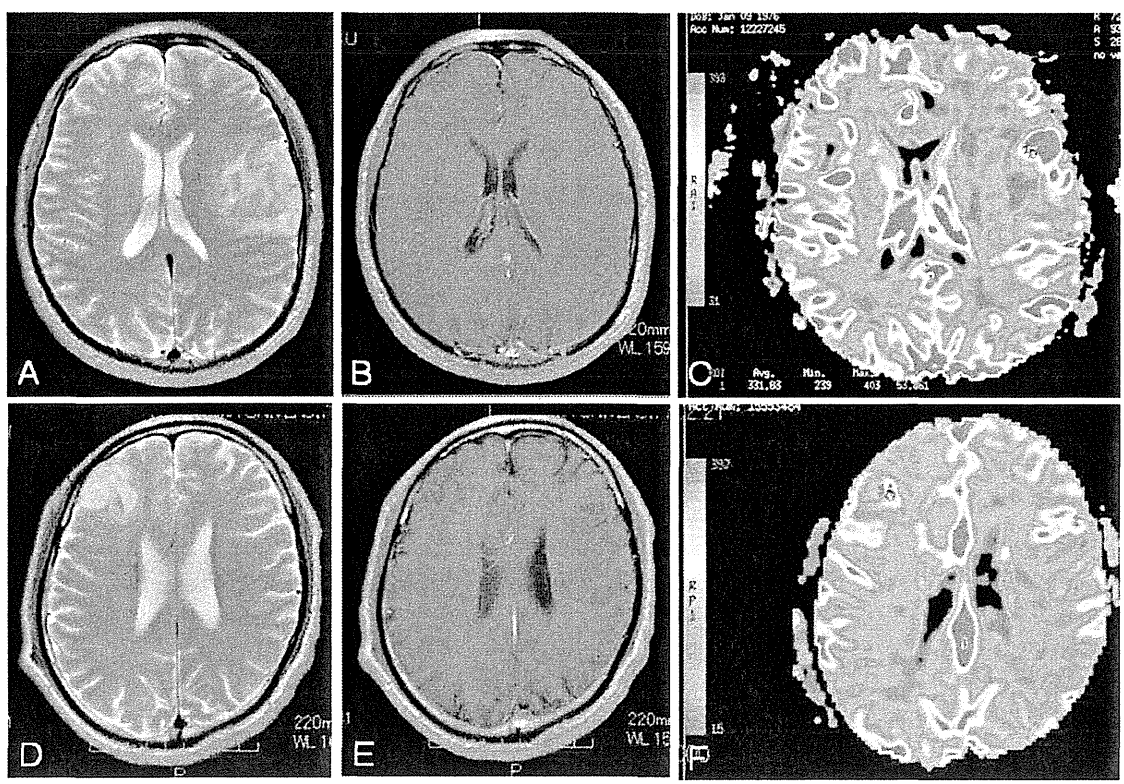

Fig. 5. (A–C) A representative case of an oligodendroglioma. (A) Axial transverse T2-weighted image shows a left frontal tumor. (B) Axial contrast-enhanced transverse T1-weighted image shows the tumor with faint partial enhancement. (C) The rCBV map shows that the rCBVmax value of the tumor is 5.12. (D–F) A representative case of an anaplastic oligodendroglioma. (D) Axial transverse T2-weighted image shows a right frontal tumor. (E) Axial contrast-enhanced transverse T1-weighted image shows the tumor without enhancement. (F) The rCBV map shows that the rCBVmax value of the tumor is 6.23.

1p/19q loss of heterozygosity. However, we did not analyze the relationship between our findings and the genetics of such tumors. In the future, further investigations aiming to correlate our findings with genetics are needed.

5. Conclusions

The present study is the first report to evaluate the role of 3 T MR PWI in differentiating between astrocytic and oligodendroglial tumors. The results showed that the rCBVmax values obtained from 3 T MR PWI may differentiate the oligodendroglial group from the astrocytic group with high sensitivity and specificity. Although only 3 T MR PWI could not clearly differentiate between these groups preoperatively, this approach may be useful as an adjunct to a post-operative histopathological diagnosis in patients presenting with gliomas.

Conflict of interest

The authors have no personal financial or institutional interest in any of the drugs, materials, or devices described in this article.

Acknowledgement

This study was supported in part by Grants-in-Aid for Scientific Research from the Ministry of Education, Culture, Sports, Science and Technology of Japan (grant no. 21791365).

References

[1] van den Bent M, Chinot OL, Cairncross JG. Recent developments in the molecular characterization and treatment of oligodendroglial tumors. Neuro Oncol 2003;5(2):128–38.
[2] Cha S, Tihan T, Crawford F, et al. Differentiation of low-grade oligodendrogliomas from low-grade astrocytomas by using quantitative blood-volume measurements derived from dynamic susceptibility contrast-enhanced MR imaging. AJNR Am J Neuroradiol 2005;26(2):266–73.
[3] Lev MH, Ozsunar Y, Henson JW, et al. Glial tumor grading and outcome prediction using dynamic spin-echo MR susceptibility mapping compared with conventional contrast-enhanced MR: confounding effect of elevated rCBV of oligodendrogliomas [corrected]. AJNR Am J Neuroradiol 2004;25(2):214–21.
[4] Maia Jr AC, Malheiros SM, da Rocha AJ, et al. MR cerebral blood volume maps correlated with vascular endothelial growth factor expression and tumor grade in nonenhancing gliomas. AJNR Am J Neuroradiol 2005;26(4):777–83.
[5] Wetzel SG, Cha S, Johnson G, et al. Relative cerebral blood volume measurements in intracranial mass lesions: interobserver and intraobserver reproducibility study. Radiology 2002;224(3):797–803.
[6] Frayne R, Goodyear BG, Dickhoff P, Lauzon ML, Sevick RJ. Magnetic resonance imaging at 3.0 Tesla: challenges and advantages in clinical neurological imaging. Invest Radiol 2003;38(7):385–402.
[7] Scarabino T, Giannatempo GM, Popolizio T, et al. 3.0-T functional brain imaging: a 5-year experience. Radiol Med 2007;112(1):97–112.
[8] Manka C, Traber F, Gieseke J, Schild HH, Kuhl CK. Three-dimensional dynamic susceptibility-weighted perfusion MR imaging at 3.0 T: feasibility and contrast agent dose. Radiology 2005;234(3):869–77.
[9] Schiffer D, Bosone I, Dutto A, Di Vito N, Chio A. The prognostic role of vessel productive changes and vessel density in oligodendroglioma. J Neurooncol 1999;44(2):99–107.
[10] Bisdas S, Kirkpatrick M, Giglio P, Welsh C, Spampinato MV, Rumboldt Z. Cerebral blood volume measurements by perfusion-weighted MR imaging in gliomas: ready for prime time in predicting short-term outcome and recurrent disease? AJNR Am J Neuroradiol 2009;30(4):681–8.
[11] Di Costanzo A, Scarabino T, Trojsi F, et al. Multiparametric 3 T MR approach to the assessment of cerebral gliomas: tumor extent and malignancy. Neuroradiology 2006;48(9):622–31.
[12] Burger PC. What is an oligodendroglioma? Brain Pathol 2002;12(2):257–9.
[13] Louis DN, Ohgaki H, Wiestler OD, et al. The 2007 WHO classification of tumours of the central nervous system. Acta Neuropathol 2007;114(2):97–109.
[14] Jeuken JW, von Deimling A, Wesseling P. Molecular pathogenesis of oligodendroglial tumors. J Neurooncol 2004;70(2):161–81.
[15] Chang SM, Nelson S, Vandenberg S, et al. Integration of preoperative anatomic and metabolic physiologic imaging of newly diagnosed glioma. J Neurooncol 2009;92(3):401–15.
[16] Cha S, Knopp EA, Johnson G, Wetzel SG, Litt AW, Zagzag D. Intracranial mass lesions: dynamic contrast-enhanced susceptibility-weighted echo-planar perfusion MR imaging. Radiology 2002;223(1):11–29.
[17] Preul C, Kuhn B, Lang EW, Mehdorn HM, Heller M, Link J. Differentiation of cerebral tumors using multi-section echo planar MR perfusion imaging. Eur J Radiol 2003;48(3):244–51.
[18] Law M, Yang S, Wang H, et al. Glioma grading: sensitivity, specificity, and predictive values of perfusion MR imaging and proton MR spectroscopic imaging compared with conventional MR imaging. AJNR Am J Neuroradiol 2003;24(10):1989–98.
[19] Arvinda HR, Kesavadas C, Sarma PS, et al. Glioma grading: sensitivity, specificity, positive and negative predictive values of diffusion and perfusion imaging. J Neurooncol 2009;94(1):87–96.
[20] Spampinato MV, Smith JK, Kwock L, et al. Cerebral blood volume measurements and proton MR spectroscopy in grading of oligodendroglial tumors. AJR Am J Roentgenol 2007;188(1):204–12.

Neurologia medico-chirurgica Advance Publication Date: November 29, 2013

ORIGINAL ARTICLE doi: 10.2176/nmc.oa2013-0112

A Multicenter Phase I/II Study of the BCNU Implant (Gliadel® Wafer) for Japanese Patients with Malignant Gliomas

Tomokazu AOKI,[1] Ryo NISHIKAWA,[2] Kazuhiko SUGIYAMA,[3] Naosuke NONOGUCHI,[4] Noriyuki KAWABATA,[4] Kazuhiko MISHIMA,[2] Jun-ichi ADACHI,[2] Kaoru KURISU,[3] Fumiyuki YAMASAKI,[3] Teiji TOMINAGA,[5] Toshihiro KUMABE,[5,†] Keisuke UEKI,[6] Fumi HIGUCHI,[6] Tetsuya YAMAMOTO,[7] Eiichi ISHIKAWA,[7] Hideo TAKESHIMA,[8] Shinji YAMASHITA,[8] Kazunori ARITA,[9] Hirofumi HIRANO,[9] Shinobu YAMADA,[10] and Masao MATSUTANI[2] for the NPC-08 study group

[1]*Department of Neurosurgery, National Hospital Organization Kyoto Medical Center, Kyoto, Kyoto;*
[2]*Department of Neuro-Oncology/Neurosurgery, Saitama Medical University International Medical Center, Hidaka, Saitama;*
[3]*Department of Neurosurgery, Graduate School of Biomedical and Health Sciences, Hiroshima University, Hiroshima, Hiroshima;*
[4]*Department of Neurosurgery, Kitano Hospital, Osaka, Osaka;*
[5]*Department of Neurosurgery, Tohoku University Graduate School of Medicine, Sendai, Miyagi;*
[6]*Department of Neurosurgery, Dokkyo Medical University Hospital, Shimotsuga, Tochigi;*
[7]*Department of Neurosurgery, Faculty of Medicine, University of Tsukuba, Tsukuba, Ibaraki;*
[8]*Department of Neurosurgery, Faculty of Medicine, University of Miyazaki Hospital, Miyazaki, Miyazaki;*
[9]*Department of Neurosurgery, Graduate School of Medical and Dental Sciences, Kagoshima University, Kagoshima, Kagoshima;*
[10]*Nobelpharma Co., Ltd., Tokyo;*
[†]*Department of Neurosurgery, Kitasato University School of Medicine, Sagamihara, Kanagawa (current affiliation)*

Abstract

Carmustine (BCNU) implants (Gliadel® Wafer, Eisai Inc., New Jersey, USA) for the treatment of malignant gliomas (MGs) were shown to enhance overall survival in comparison to placebo in controlled clinical trials in the United States and Europe. A prospective, multicenter phase I/II study involving Japanese patients with MGs was performed to evaluate the efficacy, safety, and pharmacokinetics of BCNU implants. The study enrolled 16 patients with newly diagnosed MGs and 8 patients with recurrent MGs. After the insertion of BCNU implants (8 sheets maximum, 61.6 mg BCNU) into the removal cavity, various chemotherapies (including temozolomide) and radiotherapies were applied. After placement, overall and progression-free survival rates and whole blood BCNU levels were evaluated. In patients with newly diagnosed MGs, the overall survival rates at 12 months and 24 months were 100.0% and 68.8%, and the progression-free survival rate at 12 months was 62.5%. In patients with recurrent MGs, the progression-free survival rate at 6 months was 37.5%. There were no grade 4 or higher adverse events noted due to BCNU implants, and grade 3 events were observed in 5 of 24 patients (20.8%). Whole blood BCNU levels reached a peak of 19.4 ng/mL approximately 3 hours after insertion, which was lower than 1/600 of the peak BCNU level recorded after intravenous injections. These levels decreased to less than the detection limit (2.00 ng/mL) after 24 hours. The results of this study involving Japanese patients are comparable to those of previous studies in the United States and Europe.

Key words: BCNU implant, Gliadel® Wafer, malignant gliomas, phase I/II study, pharmacokinetic

Received April 4, 2013; Accepted July 17, 2013

Introduction

Malignant gliomas (MGs) are highly malignant cancers with 5-year survival rates of 25% or less.[1] The outcomes of MG treatments have been unsatisfactory, and drugs available in Japan for the treatment of MGs are limited to certain chemotherapeutic agents such as temozolomide (TMZ, Temodar®; Merck, Whitehouse Station, New Jersey, USA). There is no standard method for the treatment of recurrent MGs.

A BCNU implant is a controlled-release preparation of carmustine (BCNU; an alkylation agent of the nitrosourea family) that is inserted into the brain. BCNU was first approved in 1979 in the United States (USA) for the treatment of multiple myeloma and other conditions. Because this drug is highly lipid-soluble and can cross the blood-brain barrier effectively, it has been used primarily by injection for the treatment of brain tumors in USA and Europe.

Conventional BCNU preparations were effective against brain tumors; however, increasing the dose level to achieve a higher efficacy caused severe adverse systemic reactions (bone marrow suppression, lung toxicity, etc.). A BCNU implant is a sterile disc-like formulation (approximately 14.0 mm in diameter and approximately 1.3 mm in thickness) containing BCNU. Under moisture-rich conditions, the biodegradable component of the preparation is gradually hydrolyzed leading to release of the active ingredient BCNU, which exerts an anti-tumor effect (Fig. 1). If this preparation is inserted in the vicinity of residual tumor tissue during surgical resection of MGs, the tumor cells can be directly and efficiently exposed to high levels of BCNU for a certain period of time starting immediately after surgery while avoiding bone marrow suppression, lung toxicity, and other negative effects. This preparation is thus expected to be beneficial for diminishing residual tumors and suppressing tumor growth. In a placebo-controlled, double-blind comparative study of patients with recurrent MGs, Brem et al.[2] reported that the cumulative death rate of glioblastoma (GBM) patients during the 6-month post-BCNU implant period was significantly lower than that in the placebo group (P = 0.013). In a placebo-controlled, double-blind comparative study of patients with newly diagnosed MGs, Valtonen et al.[3] reported that the survival rates of patients receiving BCNU implants were significantly higher than those of patients in the placebo group during the 12-month implant insertion period (P = 0.029). Westphal et al.[4] reported that the survival period was extended significantly by this preparation (P = 0.027). In these studies, the safety profile of BCNU implants was comparable to that of placebo, and no severe adverse events (bone marrow suppression, pulmonary fibrosis, etc.) due to BCNU implants were noted. On the basis of these clinical results, the BCNU implant is now recommended as an additional postoperative therapy for MGs in the treatment guidelines prepared by the National Comprehensive Cancer Network[5] and The National Cancer Institute (USA)[6] as well as the treatment guidelines prepared by the National Institute for Health and Clinical Excellence (UK).[7] However, in these clinical studies, radiotherapy was primarily utilized as concomitant therapy after BCNU implantation. These clinical studies were conducted between 1990 and 2002, and during that period, TMZ was approved only for the treatment of recurrent anaplastic astrocytoma. Therefore, combined therapy involving TMZ plus radiotherapy for newly diagnosed cases was not approved. In recent years, TMZ is often used as the standard therapy for MGs in combination with radiotherapy, and bevacizumab (BEV, Avastin®; Genentech, San Francisco, California, USA), an antivascular endothelial growth factor antibody. Therefore, it has recently been attracting attention as a new potential treatment for recurrent MGs. Retrospective reports on the safety and efficacy of BCNU implants in combination with these new treatments is available, but no prospective study has been carried out in compliance with Good Clinical Practice. Furthermore, the BCNU exposure level *in vivo* and the timing of its disappearance following insertion into the brain remain unknown. To evaluate the efficacy, safety, and pharmacokinetics of the BCNU implant combined with chemotherapy and radiation therapy after its insertion into the removal cavity in Japanese patients with MGs (newly diagnosed MGs and recurrent GBM), a prospective, uncontrolled, open-label, multicenter phase I/II study (NPC-08 study) was carried out from 2009

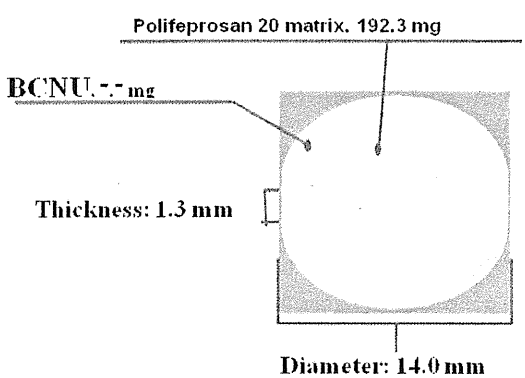

Fig. 1 BCNU implant configuration.